Earth Surf. Dynam. Discuss., doi:10.5194/esurf-2017-29, 2017
Manuscript under review for journal Earth Surf. Dynam.
Discussion started: 15 May 2017

Earth Surface Dynamics Discussions
Open Access
EGU

Model predictions of long-lived storage of organic carbon in river deposits

Mark A. Torres[1], Ajay B. Limaye[2], Vamsi Ganti[3], Michael P. Lamb[1], A. Joshua West[4], and Woodward W. Fischer[1]

[1]Division of Geological & Planetary Sciences, California Institute of Technology
[2]Department of Earth Sciences, University of Minnesota, 2 SE 3rd Ave., Minneapolis, MN 55414
[3]Department of Earth Science & Engineering, Imperial College
[4]Department of Earth Sciences, University of Southern California

Correspondence to: Mark A. Torres (mtorres@caltech.edu)

Abstract.

The mass of carbon stored as organic matter in terrestrial systems is sufficiently large to play an important role in the global biogeochemical cycling of CO_2 and O_2. Field measurements of radiocarbon-depleted particulate organic carbon (POC) in rivers suggest that terrestrial organic matter persists in surface environments over millennial (or greater) timescales, but the exact mechanisms behind these long storage times remain poorly understood. To address this knowledge gap, we developed a numerical model for the radiocarbon content of riverine POC that accounts for both the duration of sediment storage in river deposits as well as the effects of POC cycling. We specifically target rivers because sediment transport defines the maximum amount of time organic matter can persist in the terrestrial realm and river catchment areas are large relative to the spatial scale of variability in biogeochemical processes.

Our results show that rivers preferentially erode young deposits, which, at steady-state, requires that the oldest river deposits are stored for longer than expected for a well-mixed sedimentary reservoir. This geometric relationship can be described by an exponentially-tempered power-law distribution of sediment storage durations, which allows for significant aging of biospheric POC. While OC cycling partially ameliorates the effects of sediment storage, the consistency between our model predictions and a compilation of field data highlights the important role of storage in setting the radiocarbon content of riverine POC. The results of this study imply that the controls on the terrestrial OC cycle are not limited to the factors that affect rates of primary productivity and respiration, but also include the dynamics of terrestrial sedimentary systems.

Earth Surf. Dynam. Discuss., doi:10.5194/esurf-2017-29, 2017
Manuscript under review for journal Earth Surf. Dynam.
Discussion started: 15 May 2017

Earth Surface Dynamics Discussions
Open Access
EGU

1 Introduction

Terrestrial organic matter present in the biosphere, soils, and other shallow sedimentary deposits represents an enormous reservoir of carbon (4 to 5 $\times$ 10^{12} tonnes C; Fischlin et al., 2007) whose dynamics influence atmospheric O_2 and CO_2 concentrations over annual (Keeling, 1960; Keeling and Shertz, 1992; Stallard, 1998) to geologic timescales (Bird et al., 1994; France-Lanord and Derry, 1997). Understanding the links between terrestrial organic carbon (OC) cycling and atmospheric O_2 and CO_2 concentrations requires knowledge of the timescales over which OC persists in the environment before being oxidized (Berner, 1989) as well as the underlying processes that set these timescales. Identifying these processes and timescales is challenging because existing measurements of OC lifetimes show scale-dependence (i.e., the measured rate of organic carbon oxidation decreases with increasing measurement timescale; Middelburg 1989; Katsev and Crowe 2015). Consequently, measurements of terrestrial OC cycling need to made at large spatial and temporal scales to be quantitatively linked to global biogeochemical cycles.

Large rivers integrate the dynamics of OC cycling at spatial and temporal scales large enough to relate to global biogeochemical cycles. Rivers transport particulate OC (POC) eroded from across their catchment areas to the ocean, where POC is either oxidized or buried in marine sediments (Blair and Aller, 2012). Thus, rivers set the amount of time POC can persist within the terrestrial realm and integrate over areas that are large compared to the spatial scales of variability in biogeochemical processes. Annually, rivers transport large masses of POC to the ocean (1 to 2 $\times$ 10^8 tonnes C yr^{-1}; Galy et al., 2015), making fluvial transport a relevant carbon cycle flux over a range of timescales.

At the scale of river catchments, radiocarbon (^{14}C) provides a natural tracer of the lifetime of OC in surface environments. Previous studies have measured large variations in the $^{14}C/^{12}C$ of riverine POC (Masiello and Druffel, 2001; Martin et al., 2013; Clark et al., 2013; Tao et al., 2015), including significant variations in $^{14}C/^{12}C$ with depth in river channels (Galy et al., 2008; Bouchez et al., 2014). Direct interpretation of measured $^{14}C/^{12}C$ in terms of ages would imply that most riverine POC is old (thousands to tens of thousands of years). However, much of the variation in $^{14}C/^{12}C$ has been interpreted in the context of variable admixtures of two carbon components: radiocarbon-bearing organic compounds synthesized within the river catchment ("biospheric" POC) and radiocarbon-dead organics derived from the erosion of ancient sedimentary rocks ("petrogenic" POC; Masiello and Druffel 2001; Galy et al. 2008).

The erosion of petrogenic POC need not affect the atmospheric budgets of CO_2 and O_2 unless it is oxidized during transit (Bouchez et al., 2010), which releases CO_2 to and consumes O_2 from the atmosphere. Conversely, biospheric POC is a sink for CO_2 and source of O_2 over the course of its lifetime, which is thought to vary widely between different compound classes and environments (Schmidt et al., 2011). While the lifetime of biospheric POC should be reflected in its $^{14}C/^{12}C$, determining this ratio from bulk radiocarbon measurements of riverine sediments may be complicated

Earth Surf. Dynam. Discuss., doi:10.5194/esurf-2017-29, 2017
Manuscript under review for journal Earth Surf. Dynam.
Discussion started: 15 May 2017

Earth Surface Dynamics Discussions Open Access EGU

by the mixing of biospheric POC ($^{14}C/^{12}C \leq$ atmospheric ratio) with petrogenic POC ($^{14}C/^{12}C$ = 0).

Compound-specific radiocarbon analyses of terrestrial biomarkers, which can be interpreted as dominantly reflecting the biospheric component, suggest that biospheric POC has a substantially lower $^{14}C/^{12}C$ than the atmosphere in some large river systems (Galy and Eglinton, 2011; Feng et al., 2013; Tao et al., 2015; Schefuß et al., 2016). These observations require that some biospheric POC is stored in terrestrial reservoirs over (at least) millennial timescales before being transported to ultimate depocenters in marine basins. It is reasonable to ask if these observations of aged biospheric POC in modern rivers result, at least in part, from transient storage in river sediment deposits (Galy and Eglinton, 2011; Feng et al., 2013; Tao et al., 2015; Schefuß et al., 2016).

To investigate how storage in river deposits influences the ^{14}C content of riverine POC, we developed a numerical model that explicitly accounts for the effects of both sediment storage and OC cycling. The sediment storage component of our model is focused on how the stochastic nature of fluvial processes leads to the preferential recycling of young sediment deposits (Nakamura and Kikuchi, 1996; Bradley and Tucker, 2013), which, at steady-state, requires that the oldest floodplain deposits are stored for longer than expected for a well-mixed sedimentary reservoir (Bolin and Rodhe, 1973; Bradley and Tucker, 2013). This geometric relationship engenders a heavy-tailed (power-law) distribution of sediment storage durations that may allow for the significant aging of biospheric POC during storage in river deposits and impart a characteristic shape to the distribution of POC ages measured in rivers. However, the production and consumption of POC during floodplain storage can modify POC ages and may serve to ameliorate the effects of sediment storage on the POC age distribution. By including both fluvial and biogeochemical processes, our approach provides new insights into the interpretation of the terrestrial OC cycle and the radiocarbon content of riverine POC.

Starting from a generic theory for predicting the duration of sediment storage in river systems (Section 2.1), we developed a sediment storage model based on the dynamics of meandering rivers (Sections 2.2 and 2.3). We coupled this sediment storage model to a biogeochemical cycling model (Section 2.4) in order to build a full model for predicting the radiocarbon content of riverine POC under different sedimentary and biogeochemical scenarios. Predictions generated using this coupled model were compared with a compilation of field data from diverse global sites, demonstrating that the dynamics of sediment storage in shallow deposits have significant predictive skill in explaining–at least in part–the radiocarbon content of organic matter observed within many rivers (Section 3.3.1).

Earth Surf. Dynam. Discuss., doi:10.5194/esurf-2017-29, 2017
Manuscript under review for journal Earth Surf. Dynam.
Discussion started: 15 May 2017

2 Model development

2.1 Generic theory for organic carbon and sediment storage

After being eroded from an upland source, fluvial sediments are routed through a transport network that includes multiple temporary storage reservoirs (e.g., channel and floodplain deposits; Malmon et al., 2003; Lauer and Parker, 2008a; Lauer and Willenbring, 2010; Pizzuto et al., 2016). These sediment reservoirs can also store POC, potentially leading to a decrease in its radiocarbon content due to radioactive decay. The magnitude of this effect will depend on: 1) the duration of sediment storage and 2) the rate at which the ^{14}C content of POC changes with time. Developing simple models for these two factors forms the basis of our approach.

Sediment grains will spend some portion of their time in transient storage within sediment deposits and the remainder of their time in active transport associated with the river channel. We posit that the time spent in storage is much greater than the time spent in active transport (e.g., Sadler, 1981; Ganti et al., 2011) and, as a result, that the total transit time of sediments from source to sink can be approximated as the total time spent in storage. Since sediment grains likely enter and exit temporary storage reservoirs multiple times during transit, the total storage time can be separated into two components: 1) the number of times that grains enter and exit storage reservoirs and 2) and the duration of each storage event.

Fluvial processes are expected to cause natural variations in the duration of each storage event. This variability can be simulated by representing storage duration as a random variable with some probability distribution p_S(t). Thus, for some number of storage events n, the transit time can be calculated as the sum of n draws from the probability distribution of storage durations. Since the sediment load transported by rivers is composed of a collection of sediment grains with different storage histories, it will be characterized by some distribution of transit times that reflects both p_S(t) as well as the total number of storage events. Mathematically, the transit time distribution (p_{Tr}(t)) is given by the convolution of the storage distribution by itself n times

$$p_{Tr}(t) = p_S(t)^{*n} \tag{1}$$

To predict the change in the radiocarbon content of POC that results from sediment storage, the functional relationship between the radiocarbon content of POC and time, $f(t)$, can be used to transform the transit time distribution into a distribution of radiocarbon contents (p$_F$(^{14}C)) where:

$$p_F(^{14}C) = p_{Tr}(f^{-1}(t))\frac{dt}{d^{14}C} \tag{2}$$

We note that $f(t)$ need not be the radioactive decay equation if POC is continuously produced and consumed during fluvial transit, which is considered in greater detail in Section 2.4.2.

Earth Surf. Dynam. Discuss., doi:10.5194/esurf-2017-29, 2017
Manuscript under review for journal Earth Surf. Dynam.
Discussion started: 15 May 2017

2.2 Application of a meandering model to determine storage duration

Identifying appropriate mathematical expressions for the probability distribution of storage durations is critical to developing realistic models for several geochemical tracers in river sediments, including the radiocarbon content of POC, that have nonlinear changes in concentration with time. Most previous models of sediment storage in meandering river systems have assumed that storage durations are exponentially distributed (Malmon et al., 2003; Lauer and Parker, 2008a; Lauer and Willenbring, 2010). This assumption requires that deposits of all ages are equally likely to be eroded at any given time, which is inconsistent with some field data (Nakamura and Kikuchi, 1996; Lancaster and Casebeer, 2007) as well as the common observation that the position of the river channel is persistent in time (Bradley and Tucker, 2013). To develop a more realistic storage duration distribution, it is necessary to consider the physical processes that govern sediment exchange in natural river systems.

In lieu of following a static path, many rivers migrate laterally across their floodplains with time. Single-thread, migrating (i.e., meandering) channels are one of the most common channel types and show morphodynamic processes common to all alluvial rivers (Dunne and Aalto, 2013). Over time, lateral migration of single-thread rivers leads to the development of arcuate meander bends. Meander bends can grow until a cutoff event occurs where the river bypasses an existing portion of its reach in favor of a straighter path (e.g., Hooke, 1995). Together, lateral migration and cutoff allow rivers to traverse back and forth across their floodplains over time and continuously exchange sediments in active transport with those in passive storage. Thus, the spatial and temporal patterns of lateral migration and cutoff directly impact the duration of sediment storage in fluvial systems (Bradley and Tucker, 2013).

In order to capture the full range of relevant time and space scales, which are inaccessible in field observations of lateral migration (Black et al., 2010; Constantine et al., 2014), we used an existing numerical model of river meandering (Howard and Knutson, 1984; Limaye and Lamb, 2013) to derive a process-based probability distribution of storage durations. The meandering model assumes a fixed channel width and represents the channel position using a series of discrete nodes. At each node, local rates of relative channel migration depend upon the local and upstream-weighted channel curvature. Local rates of lateral migration are then computed from the relative channel migration rate, sinuosity, and a user-defined bank erodibility coefficient, which sets average lateral migration rate for each simulation. Neck cutoffs occur whenever the channel intersects itself; chute cutoffs are not modeled. We fixed the maximum channel lateral erosion rate at 0.05 channel widths per year, which is typical for actively migrating meandering rivers (e.g., Hickin and Nanson, 1975; Constantine et al., 2014), and ran each model simulation for a total of 10^5 years. In the model topology, the channel is inset in a planar floodplain surface and migrates laterally with no bed elevation change. We neglect over bank deposition and the loss of sediment due to subsidence, but discuss these in Section 4.1. A schematic of the model is shown in Figure 1.

Earth Surf. Dynam. Discuss., doi:10.5194/esurf-2017-29, 2017
Manuscript under review for journal Earth Surf. Dynam.
Discussion started: 15 May 2017

The numerical model runs yield a time-series of channel positions. For all timesteps, we define areas within the active channel as having a sediment age of zero. As time proceeds and the channel migrates, it abandons sediments along the inner bank (i.e., point bar deposits), which begin to age. When the active channel overlaps existing deposits, the time elapsed since the emplacement of those deposits is recorded as the storage duration. Since areas bounded by the channel are defined as having a sediment age of zero, the model does not allow for cumulative aging as a result of multiple deposition and transport events (i.e., once material is eroded, its age is reset to zero). As a consequence, the model does not measure the total amount of time sediments spend in storage (transit time), but instead tracks the amount of time spent in storage for a single deposition/erosion event (storage duration).

Using the time-series of channel positions, we calculated storage durations as the ages of river deposits that are eroded by lateral migration at each time step. The storage duration for each eroded deposit is weighted by its areal extent along the active channel, and observations from each timestep were combined to yield a full distribution of storage durations for the model. We note that excluding data from the beginning (e.g., the first 50%) of the model runs does not significantly affect the full distribution since short storage durations are more probable overall. We also examined the age distribution of deposits remaining on the floodplain at the end of the model run, which we termed the deposit age distribution.

Our approach of using a numerical model of river meandering is similar to that of Bradley and Tucker (2013), who developed a quasi-static storage duration distribution from a single meandering model simulation. The river meandering model used in this study (Howard and Knutson, 1984) differs from the Lancaster and Bras (2002) model used by Bradley and Tucker (2013). A salient difference between the models is that only the Lancaster and Bras (2002) model has been shown to develop compound bends prior to cutoff. However, similar bend geometries rapidly develop in the Howard and Knutson (1984) model due to meander cutoff. Also, compared to Bradley and Tucker (2013), our analysis uses a suite of model runs with boundary conditions that allow freer channel motion (e.g., the model uses a fixed upstream boundary condition, which limits drift of the mean channel axis; Limaye and Lamb, 2013). To systematically account for the sensitivity of the meandering model to the initial conditions, which can impact modeled river trajectories (e.g., Frascati and Lanzoni, 2009), we used five replicate simulations to determine storage duration distributions and fifty replicate simulations to determine deposit age distributions.

2.2.1 Scaling model results to natural systems

Our meandering model simulations should capture the appropriate shape of the storage duration distribution. However, absolute values should vary as a function of the lateral migration rate. Specifically, rivers that migrate quickly should have, on average, shorter storage durations relative to rivers that migrate slowly. In order to account for the effects of variable migration rates, we normalized all

Earth Surf. Dynam. Discuss., doi:10.5194/esurf-2017-29, 2017
Manuscript under review for journal Earth Surf. Dynam.
Discussion started: 15 May 2017

storage durations by the time required for the channel to migrate laterally to the point of meander bend cutoff (T_{cut}). By explicitly tracking bends from growth to cutoff (Schwenk et al., 2015), we find that T_{cut} is equal to 350 years in our meandering model simulations. Normalizing the meandering model results by this T_{cut} value yields a dimensionless storage duration distribution that can be re-scaled to produce variable sediment storage times by varying T_{cut}.

To aid in model-data comparisons, it is useful to develop a prediction for how T_{cut} may vary between river systems. Based on a separate set of meandering model runs with variable maximum lateral migration rates (0.0005 to 0.05 channel widths per year), we found that T_{cut} is proportional to the inverse of the maximum lateral migration rate such that

$$T_{cut} = c_1 \times \left(\frac{w}{E_{L,max}}\right) \tag{3}$$

where w is the channel width (meters), $E_{L,max}$ is the maximum lateral migration rate (meters year^{-1}) and c_1 is an empirical constant equal to 13.6 $\pm$ 3.3 (Figure 2a). Maximum lateral migration rates ($E_{L,max}$) are used for this comparison because they are specified in the model runs; average rates are typically a factor of about 3 lower.

Field compilations show that mean lateral migration rates are positively correlated with sediment fluxes (Q_s; Figure 2; Aalto et al., 2008; Grenfell et al., 2012; Constantine et al., 2014). This correlation may reflect the fact that in order for the river channel to migrate by one channel width, sufficient sediment must be supplied so that a deposit of equivalent volume is created. Along a meander bend, the volume of the sediment deposit produced after a river migrates one channel width should be proportional to the product of the bend wavelength (λ), channel depth (h), and channel width (w). In field data (e.g., Williams, 1986), both λ and h are correlated with w such that the deposit volume can be approximated as being proportional to w^3. In Figure 2, the correlation between lateral migration rates and sediment fluxes (Constantine et al., 2014) is recast in terms two timescales: the time required to migrate one channel width (w/E_L) and the time required to supply a proportional volume of sediment (w^3/Q_s). Taken all together, the correlations depicted in Figure 2a-b imply that relative T_{cut} values can be determined for field systems through comparison of w^3/Q_s. That is, natural rivers with higher w^3/Q_s appear to migrate more slowly and therefore store sediments for longer.

2.3 Model for the number of storage events

Following the generic theory presented in Section 2.1, the sediment transit time is equal to the sum of independent draws from the storage duration distribution with the number of independent draws being equal to the total number of storage events (Equation 1). Thus, calculating transit time distributions (TTDs) from the storage duration distribution requires a model for the total number of storage events sediment undergoes during riverine transit.

Following previous approaches (e.g, Malmon et al. 2003; Lauer and Parker 2008b; Pizzuto et al. 2014), we defined a characteristic length scale over which eroded sediment particles are transported

Earth Surf. Dynam. Discuss., doi:10.5194/esurf-2017-29, 2017
Manuscript under review for journal Earth Surf. Dynam.
Discussion started: 15 May 2017

before being re-deposited. While particles are transported variable distances (depending for example on particle size and current velocity), we made the simplifying assumption that the dispersion of the distribution of transport lengths is small relative to the mean transport length. We defined the characteristic transport length (x_{tran}) by balancing the flux of sediment carried downstream with the lateral flux of sediment that results from channel migration. In this way, x_{tran} represents the length of channel required to exchange the entire sediment flux with river deposits via lateral migration. This definition of x_{tran} is comparable to previous studies (Malmon et al., 2003; Lauer and Parker, 2008b; Pizzuto et al., 2014) and was calculated with the equation:

$$x_{\text{tran}} = \frac{Q_s}{E_L \times h} \tag{4}$$

where Q_s is the volumetric sediment flux ($m^3\ yr^{-1}$), E_L is the mean lateral migration rate ($m\ yr^{-1}$), and h is the channel depth (m). The appropriate number of transport events (n_x) can be determined by taking the nearest integer of the ratio of the total channel length to x_{tran}. The sediment transit time distribution can then be determined by convolving the storage duration distribution with itself n_x times (Equation 1).

2.3.1 Prediction of downstream changes

By relating the number of transport events to a characteristic length scale (Equation 4), our model predicts an increase in transit times as sediments are transported downstream. This relationship between channel length and transit time forms the basis of our comparison between model results and field data as it allows datasets without direct measurements of sediment transit times to be used. Correlations apparent in field data (Figure 2b) imply that variations in x_{tran} should be minimal between river systems such that variations in channel length are the dominant control on n_x (see Equation 4). Here, we set x_{tran} equal to 100 km, which is close to the mean x_{tran} (109±68 km) calculated from the data compilation shown in Figure 2c and agrees with a complementary, but independent, analysis by Pizzuto et al. (2016), which suggests that particles enter and exit storage reservoirs 10 times as they transit along a 1000 km long channel.

The predicted changes in sediment transit times with increasing transport length can be cast in terms of catchment area by taking advantage of the power-law relationship between channel length (L; km) and catchment area (A; km^2; Hack, 1957). This relationship is useful because catchment areas have been reported for all field data within our compilation (see Section 2.5). We transformed modeled channel lengths using the equation:

$$L = 1.4 \times A^{0.5} \tag{5}$$

The value of the exponent selected (0.5) reflects a compromise between small (< 2×10^5 km^2) and large (> 2×10^4 km^2) river catchments, which are characterized by larger (0.6) and smaller (0.47) exponents, respectively (Mueller, 1973). To model catchments with channel lengths shorter than

Earth Surf. Dynam. Discuss., doi:10.5194/esurf-2017-29, 2017
Manuscript under review for journal Earth Surf. Dynam.
Discussion started: 15 May 2017

x_{tran}, we assumed they have a mixture of POC with a zero age and POC aged by one transport event. The relative proportion of aged material is equal to the ratio of the channel length to x_{tran}.

2.4 Linking sediment transit times to POC ages

2.4.1 End-member case with zero cycling

To link our prediction of sediment transit time distributions (TTDs) to POC ages, we started by assuming that the age distribution of POC is equal to the sediment TTD. This can be conceptualized as a system where sediments from a source area contain an initial amount of POC with a zero age. The POC and sediments from the source area then transit through a floodplain with no subsequent POC oxidation or production. This simplified approach serves as a useful end-member case where POC increases in age as much as allowed by sediment storage. To contrast with this, section 2.4.2 describes an approach that explicitly incorporates the effects of POC cycling into the prediction of POC age distributions.

The radiocarbon content of riverine POC is often used as a tracer of the timescale of POC cycling. Typically, radiocarbon measurements are reported as the fraction modern (Fm), which is defined as:

$$Fm = \left(\frac{^{14}C}{^{12}C}_{sample*}\right) / \left(\frac{^{14}C}{^{12}C}_{modern}\right) \tag{6}$$

where the subscript sample* refers to the ratio of ^{14}C to ^{12}C in a sample normalized to a fixed ^{13}C to ^{12}C ratio (δ^{13}C = -25 ‰) and the subscript modern refers to the ^{14}C to ^{12}C ratio of a standard. Unlike calendar ages, Fm mixes linearly, making it appropriate for use in systems where POC is composed of a mixture of components with different ages.

Assuming conservative behavior of POC, the appropriate function to transform the sediment transit time distribution into a distribution of Fm values (Equation 2) is the radioactive decay equation:

$$Fm = e^{-\lambda t} \tag{7}$$

where λ is the ^{14}C decay constant (1.201×10^{-4} year^{-1}). Here, we assumed that the ^{14}C/^{12}C ratio of the atmosphere is constant in time in order to simplify the model and focus on the role of sediment transport dynamics in setting the radiocarbon content of riverine POC.

2.4.2 Modeling POC cycling in floodplains

If POC is produced and/or consumed during floodplain storage, its age will not be exactly equal to the age of the sediment deposit in which it occurs. If, for example, new POC is produced as older POC is consumed, then the radiocarbon content of bulk POC will increase and be shifted to younger ages relative to the sediment deposit. Production and consumption of POC during sediment storage is consistent with existing radiocarbon measurements from soil chronosequences. Importantly,

Earth Surf. Dynam. Discuss., doi:10.5194/esurf-2017-29, 2017
Manuscript under review for journal Earth Surf. Dynam.
Discussion started: 15 May 2017

soil chronosequence studies from environments where the parent material contains little to no petrogenic POC show a general decrease in the Fm of biospheric POC with deposit age (Torn et al., 1997; Lawrence et al., 2015). This relationship implies that, even with active POC cycling, sediment storage will affect the age distribution of riverine POC.

Including the effects POC cycling in our modeling framework requires a description of the kinetics of POC production and consumption. We adopted a simple approach in order to demonstrate the general effects of POC cycling (based on Jenny et al., 1949). This model assumes that the time rate of change in the POC content of a sediment deposit depends on the balance between POC production and consumption. For simplicity, POC consumption is assumed to be first-order with respect to POC concentrations, which yields the equation

$$\frac{dC}{dt} = P - k(C) \tag{8}$$

where C is the POC concentrations (g cm^{-3}), P is the production rate (g cm^{-3} yr^{-1}), and k is the consumption rate constant (yr^{-1}). This equation predicts that the concentration of POC within a sediment deposit increases with time until it reaches a steady-state concentration equal to P/k. The e-folding time of this increase is equal to $1/k$.

To incorporate radiocarbon (as Fm) into this model, it is necessary to write separate versions of Equation 8 for ^{12}C and ^{14}C. For ^{14}C, an additional term is required to account for radioactive decay, which yields the equation:

$$\frac{d^{14}C}{dt} = {}^{14}P - k(^{14}C) - \lambda(^{14}C) \tag{9}$$

When combined with Equation 8, Equation 9 predicts that the Fm of biospheric POC decreases with time to a steady-state value equal to $(k \times R)/(\lambda + k)$ where R is the ratio of the production rate of ^{14}C to the production rate of ^{12}C. For constant steady-state concentrations of POC, the time required for the system to reach steady-state with respect to Fm scales negatively with the POC consumption rate constant (i.e., systems with more slowly cycling carbon require more time to reach a steady-state).

Equations 8 and 9 can be integrated from the minimum to maximum sediment transit time in order to simulate the evolution of POC concentrations (Equation 8) and Fm (ratio of Equations 8 and 9) with time for different POC production and consumption rates. These integrated equations can be used to transform the storage duration distribution into a distribution of POC concentrations and Fm for one transport event (Equation 2). To model additional transport events, the means of the concentration and Fm (weighted by concentration) distributions from the preceding transport event were set as the initial values for the integrated forms of Equations 8 and 9 used to transform the storage duration distribution. We used this method to account for in-channel mixing, which will tend to homogenize POC in between transport events. Note that the Fm values modeled in this manner are not strictly "ages" in any meaningful way, but instead represent the Fm that results from a dynamic balance between POC production, consumption, and radioactive decay.

Earth Surf. Dynam. Discuss., doi:10.5194/esurf-2017-29, 2017
Manuscript under review for journal Earth Surf. Dynam.
Discussion started: 15 May 2017

2.4.3 Accounting for the chemical heterogeneity of POC

Applying Equations 8 and 9 requires specifying values for the POC production rate and consumption rate constant. Natural OC is a compositionally heterogeneous material, and cannot be described by single values for these parameters due to differing rates of biological production and/or resistance to (bio)degradation. To account for this expected heterogeneity, Equations 8 and 9 can sum across multiple POC "pools" with differing production rates (P) and consumption (k) rate constants (Jørgensen, 1978; Berner, 1980; Boudreau and Ruddick, 1991). For POC concentrations, this can be written as:

$$\frac{dC}{dt} = \sum_{i=1}^{j} P_i - k_i(C_i) \tag{10}$$

where i represents an individual POC pool and j is the total number of POC pools. An analogous equation can be written for ^{14}C by adding the term for radioactive decay for each POC pool.

Applying Equation 10 requires specifying the number of POC pools as well as their individual steady-state concentrations and consumption rate constants. A simple version of such a model involves two POC pools (j = 2): "fast" cycling POC and "slow" cycling POC. The fast cycling POC pool has a higher steady-state concentration and a higher consumption rate constant relative to the slow cycling pool. As a result, POC concentrations are dominated by the fast pool while Fm values are more sensitive to the slow cycling pool.

Using the sediment TTDs we developed, we calculated the bulk radiocarbon content of riverine POC using different parameter values of the 2-pool POC cycling model. In all models, the fast cycling POC pool had a fixed consumption rate constant of 0.01 yr^{-1} As long as the rate constant for fast cycling POC is greater than 0.001 yr^{-1}, its value has little affect on the model results as this pool cycles rapidly enough to maintain a $Fm \approx$1. To produce POC with a low Fm value, we set the rate constant describing the slow cycling POC pool to either 2×10^{-6} or 2×10^{-5} yr^{-1}. Production rates of fast POC were fixed to produce a steady-state concentration of fast POC equal to 0.1 g cm^{-3}. Production rates of slow POC were varied such that the steady-state concentration of slow POC was between 5 and 80% of the total (fast + slow) steady-state POC concentration. While consistent with some available field data (e.g., Middelburg, 1989), these parameter values were largely selected in order to produce the range of biospheric Fm values observed in natural rivers (see Section 2.5 below).

2.5 Field data compilation and analysis

To benchmark our model results, we compiled field data on the radiocarbon content of riverine POC. As previously mentioned, the bulk radiocarbon content of riverine POC is strongly affected by the mixing of biospheric POC ($Fm \leq 1$) with petrogenic POC (Fm=0). Since our model predicts only the change in the radiocarbon content of biospheric POC, it is necessary that we correct for the

Earth Surf. Dynam. Discuss., doi:10.5194/esurf-2017-29, 2017
Manuscript under review for journal Earth Surf. Dynam.
Discussion started: 15 May 2017

proportion of petrogenic POC in field data. This is accomplished using a modified version of the Galy et al. (2008) two-component mixing model, which requires datasets with more than 2 measurements of Fm per site.

We identified 50 river systems with more than 2 measurements of the concentration and radiocarbon content of riverine POC (full reference list in Table 1). Following Galy et al. (2008), the bulk Fm measurement can be related to the proportions of petrogenic POC (POC_p) and biospheric POC (POC_b) by the equation:

$$Fm_{bulk} \times [POC]_{bulk} = (Fm_b \times [POC]_b) + (Fm_p \times [POC]_p) \tag{11}$$

where [POC] is the concentration of POC in units of g C g^{-1} sediment. If it is assumed that petrogenic POC is present at a fixed concentration in sediments, then the relationship:

$$[POC]_p = [POC]_{bulk} - [POC]_b \tag{12}$$

can be substituted into Equation 11. Since the Fm of petrogenic C is equal to zero, the assumptions stated above yield the hyperbolic equation:

$$Fm_{bulk} = \frac{Fm_b \times ([POC]_{bulk} - [POC]_p)}{[POC]_{bulk}} \tag{13}$$

All the data from each individual site in our compilation were fit with the non-linear form of the mixing equation (Equation 13) using the Trust-Region algorithm available in the MATLAB 2015a Curve Fitting Toolbox. Since Equation 13 predicts a hyperbolic relationship between POC concentrations and Fm that is concave down, we screened all of the regression results in order to identify instances where a two-component mixing model was inconsistent with the data. Of the 50 river systems in the data compilation, 21 were consistent with the two-component mixing model (Equation 13) and yielded an estimate of the Fm of bulk biospheric POC (Results shown in Table 2). Of these 21 river systems, we excluded one (The Rhône River; biospheric Fm = 1.41 $\pm$ 0.15) from further analysis due to its high Fm, which we attribute to anthropogenic contamination.

3 Results

3.1 Meandering model predictions of storage durations

Averaged across our model simulations, the probability distributions of storage durations show a power-law decay in probability as the storage duration increases (Figure 3a). We considered this to be a key feature of the meandering model results, and aimed to capture it in our statistical representation of the modeled age distributions. Without an upper bound, power law distributions can have infinite moments and thus have limited value in describing the full range of behavior of natural systems. Since river systems have a finite size and are expected to eventually recycle more or less all the sediment they store, we employed a tempered Pareto distribution (Cartea and Del-Castillo-Negrete,

Earth Surf. Dynam. Discuss., doi:10.5194/esurf-2017-29, 2017
Manuscript under review for journal Earth Surf. Dynam.
Discussion started: 15 May 2017

2007; Rosiński, 2007) to describe our model results. The tempered Pareto distribution displays a power-law decay until some upper limit where it becomes exponentially tempered. Relative to the truncated Pareto distribution (Mantegna and Stanley, 1994), which simply has a fixed cutoff at some upper limit, the tempered Pareto distribution is less restrictive as it allows the upper bound to also be a stochastic quantity.

Using the approach outlined in Meerschaert et al. (2010), we fit the dimensionless storage duration distribution determined from the meandering model simulations to a tempered Pareto distribution ($p(t)$; Figure 3a), which has a probability density function (pdf) given by:

$$p(t) = \gamma t^{-\alpha-1} \times e^{-t/\beta} \times (\alpha + t/\beta) \tag{14}$$

where t is the storage duration, γ is a scale parameter, α is a tail-index, and β is a tempering parameter. The γ parameter relates to the lower bound of the probability distribution and thus sets the minimum storage time. The α parameter describes the power-law decay in the relationship between probability and storage duration. The β parameter describes the storage duration at which power-law behavior ceases and the storage duration distribution begins to follow an exponential function. Our best-fit values of γ, α, and β are 1.2, 0.8, and 120. We used equation 14 with these values as the storage duration distribution in order to calculate the sediment TTDs used in all subsequent results (Equation 1).

At steady-state, the storage duration distribution can be uniquely related to the ages of sediment deposits remaining in storage after one transport event (Bolin and Rodhe, 1973; Bradley and Tucker, 2013). Specifically, Bradley and Tucker (2013) demonstrated that the pdf of deposit ages (p_A(t)) is proportional to the survivor function (or complementary cumulative distribution function) of storage durations ($S_S(t)$)

$$p_A(t) = \tau \times S_S(t) \tag{15}$$

where τ is a constant of proportionality that is equal to the ratio of the input/output fluxes to the total reservoir size. Given the relationship between density and survivor functions, Equations 14 and 15 make a prediction for the relationship between the tail-indices of the of the deposit age (α_d) and storage duration (α_s) distributions. Specifically, α_d = 1-α_s at steady-state. Individually fitting the results of each of our five replicate simulations yields α_s values that range from 0.8 to 1. This range of α_s values, which we assume represents the uncertainty of our estimate, predicts a range of α_d values that overlaps with our best-fit estimate of α_d from fitting Equation 14 to the deposit age distribution derived from fifty replicate model simulations (α_d = 0.1; Figure 3a). This consistency between the storage duration and deposit age distributions suggests that our model simulations were at steady-state with respect to sediment storage.

By using the tempered-Pareto distribution (Equation 14) to represent the distribution of storage durations, we excluded storage durations less than the lower bound, which is related to the γ parameter and approximately equal to one cutoff time. In our model simulations, the proportion of the

Earth Surf. Dynam. Discuss., doi:10.5194/esurf-2017-29, 2017
Manuscript under review for journal Earth Surf. Dynam.
Discussion started: 15 May 2017

age distribution with storage durations less than the lower bound is small (Figure 3a), which implies that the lower bound imposed by the tempered-Pareto distribution may not significantly effect our modeled transit time distributions. Similarly, for modeling POC cycling, a fixed lower bound may be a reasonable approximation since soil chronosequence studies imply that the onset of significant organic carbon accumulation is lagged relative to the time of sediment deposition (Torn et al., 1997; Masiello et al., 2004; Lawrence et al., 2015). Consequently, the small proportion of young sediments not included in our model is not expected to participate significantly in organic carbon cycling.

3.1.1 Non-dimensional model behavior

To show the general model behavior, we started by comparing the dimensionless sediment TTDs generated using Equations 1 and 14 for 1 to 20 transport events (Figure 3b). As expected, our calculations show that sediment ages increase with the number of transport events. They also show that the shape of the transit time distribution changes with increasing number of transport events (Figure 3c). This change in shape is due to the central limit theorem, which states that sum of independent random variables tends towards a normal distribution even when drawn from a distribution that is not normal. The central limit theorem applies in this case because the tempered-Pareto distribution has finite moments due to the exponential tempering of the longest storage durations. However, as a semi-heavy tailed distribution, sums of tempered-Pareto variables take longer to converge to a normal distribution relative to exponentially-distributed variables. As a result, sediment TTDs skewed towards older ages are expected despite the mixing effects of multiple transport events (Figure 3b,c).

The dimensionless sediment TTDs show a roughly linear increase in the mean transit time (MTT) with increasing number of transport events (Figure 3b). Assuming that x_{tran} is relatively constant, which is consistent with field data (Figure 2c), the number of transport events should increase with the ratio of the square root of catchment area to x_{tran} (Equation 5; Hack, 1957). This metric for the relative number of transport events ($\sqrt{A}/x_{tran}$) can be combined with our metric for relative T_{cut} values (w^3/Q_s; Section 2.2.1) to produce a metric for the relative transit time of sediments where:

$$\text{Relative Transit Time} = \frac{\sqrt{A}}{x_{tran}} \times \frac{w^3}{Q_s} \tag{16}$$

This simplified metric captures the expected effects of sediment supply (Constantine et al., 2014) and channel length (Malmon et al., 2003; Lauer and Parker, 2008b; Pizzuto et al., 2014) on the duration of sediment storage in river deposits and is useful for comparing systems where more direct measurements of sediment ages are unavailable.

3.2 Coupling sediment storage to POC cycling

3.2.1 Radiocarbon as a POC storage tracer

The radiocarbon content of biospheric POC is a tracer of the lifetime of POC in surface environments, which reflects both the rate of POC cycling and the duration of time over which these reac-

Earth Surf. Dynam. Discuss., doi:10.5194/esurf-2017-29, 2017
Manuscript under review for journal Earth Surf. Dynam.
Discussion started: 15 May 2017

Earth Surface Dynamics Discussions
Open Access
EGU

tions occur. For a sediment deposit with a single age, the bulk radiocarbon content (as Fm) is set by the POC production rate, the POC consumption rate constant, as well as the deposit age (Equation 9). For river sediments, which are composed of a mixture of variably-aged deposits (Figure 3), it is expected that the relationship between the bulk Fm, POC cycling parameters, and storage time will depart significantly from the behavior expected for a single-age deposit (Equation 9). The magnitude of the difference between the heterogeneous (sediment TTD) and homogeneous (single-age deposit) cases depends on the transit time distribution as well as the values of the POC consumption rate constants. The direction and magnitude of the offset is important to constrain as it underlies the quantitative interpretation of field data.

In analyzing the model predictions, we start by comparing the predicted relationships between the mean transit time (MTT) and bulk Fm for heterogeneous systems with a distribution of sediment transit times versus homogeneous systems with a single transit time. For this analysis, we re-scaled the dimensionless sediment TTDs shown in Figure 3b using T_{cut} values selected such that the MTT for each distribution shape varied between 10^3 and 10^6 years. This approach is consistent with field estimates of MTTs, which range from 10^3 to 5×10^5 years when measured using sediment budgeting (Blöthe and Korup, 2013) or radionuclide approaches (Dosseto et al., 2006; Granet et al., 2010; Wittmann et al., 2015, 2016; Li et al., 2016).

The exact difference in Fm between the heterogeneous and homogeneous cases depends on the MTT (Figure 4a). When the MTT is long relative to the time it takes OC cycling to reach steady-state, there is no difference between the Fm predicted by the heterogeneous and homogeneous models. However, when a significant portion of the sediment TTD consists of transit times less than the time required to reach steady-state with respect to OC cycling, there are significant differences between the Fm predicted by the heterogeneous and homogeneous models. For the cases considered here, these differences can approach 0.1 Fm units (Figure 4a), which is two orders of magnitude greater than typical analytical uncertainties. Consequently, applying models based on homogeneous systems (e.g., Equations 8, 9, and 10) to radiocarbon measurements of riverine POC may yield parameter values that are off by large factors relative to their true values. In particular, applying homogeneous models to riverine POC is likely to yield apparent OC cycling rates that are fast relative to the "true" rates due to the significant proportion of sediments with short transit times.

While heterogeneous sediment TTDs lead to quantitatively distinct relationships between sediment MTTs and POC Fm values, the large differences in parameter values we selected allow the OC cycling models to be distinguished from one another despite the differences induced by variable TTD shapes (Figure 4a). When there is only a very small fraction (i.e., 5%) of slow OC, bulk Fm values remain close to 1 at all MTTs (Figure 4a). Larger portions of slow OC result in more variable Fm values. For systems with identical values of POC consumption rate constants, increasing the portion of "slow" OC decreases the Fm observed at a given MTT (Figure 4a).

Earth Surf. Dynam. Discuss., doi:10.5194/esurf-2017-29, 2017
Manuscript under review for journal Earth Surf. Dynam.
Discussion started: 15 May 2017

In general, OC cycling models with lower POC consumption rate constants (i.e., slower OC cycling) have lower steady-state Fm values, but take longer to reach steady-state. As a result, for intermediate MTTs, the bulk Fm of riverine POC can have a higher value for systems with slower POC cycling rates relative to those with faster cycling rates (Figure 4a). This counter intuitive result stems from mass balance constraints within the model, which require more slowly cycling compounds to be produced at slower rates if their concentrations are to remain a fraction of the total POC concentration. In other words, for the same MTT, more slowly cycling POC produced at a slower rate can yield a similar bulk Fm to more rapidly cycling POC produced at a faster rate (Figure 4).

Results show that a single observation of the bulk Fm of riverine POC can yield a non-unique interpretation of the underlying POC cycling dynamics even if the sediment TTD is known independently (Figure 4a). While this is also true when analyzing soil POC, the chronosequence approach (i.e., analyzing soils of variable, but independently known ages from the same site) can be used to better distinguish between different models. Our analysis highlights an analogous approach that can be applied to river systems where bulk Fm values can be compared within a given river system or between similar river systems with differing sediment transit times. In our results, OC cycling rates are distinguished by the shape of the relationship between MTT and bulk Fm (Figure 4a). In principle, samples with variable MTTs can be collected from the same river system by analyzing a downstream profile of riverine POC over a length greater than the characteristic transport length scale (Equation 4).

3.3 The downstream profile of POC radiocarbon

For fixed values of POC cycling rates, the bulk Fm of riverine biospheric POC depends on the MTT (Figure 4a), which increases as the number of transport events increases (Figure 3b). Thus, our model predicts that the bulk Fm of biospheric POC should decrease downstream. The exact shape of this decrease depends on the POC cycling rates as well as the relationships between channel length and sediment transit times set by the transport length scale (x_{tran}), the number of transport events (n_x), and the cutoff time (T_{cut}).

For short channel lengths, all Fm-channel length relationships show Fm values near 1 (i.e., modern POC) due to limited storage (Figure 4b). As channel length increases, each relationship tends towards the steady-state Fm that is set by the POC consumption rate constants (Figure 4b). For each curve shown in Figure 4b, the relative increase in channel length required to reach the steady-state Fm is set by T_{cut} and x_{tran}. In other words, low Fm values require slow POC cycling rates, but these values can only be expressed with sufficient sediment storage, which increases with increasing channel length. This result illustrates that the downstream profile of the radiocarbon content of biospheric POC contains information regarding the interplay between sediment storage and OC cycling (Figure 4b).

Earth Surf. Dynam. Discuss., doi:10.5194/esurf-2017-29, 2017
Manuscript under review for journal Earth Surf. Dynam.
Discussion started: 15 May 2017

3.3.1 Benchmark with natural systems

The model results shown in Figures 4a illustrate that increasing the proportion of slow cycling POC results in a decrease in Fm, whereas decreasing the consumption rate constant can increase Fm. With this in mind, we compared our field data to POC cycling models with fixed POC consumption rate constants (fast and slow rates of 0.01 and 2×10^{-5} yr^{-1}, respectively), but variable proportions of slow POC (10%, 33%, and 80%). These OC cycling models are contrasted with an "inert" model (Section 2.4), where POC is assumed to have the same age distribution as the sediments. To produce a range of sediment MTTs, we consider simulations with T_{cut} values of 350 and 1000 years.

All field data within our compilation fall within the region defined by our model predictions after taking into account the uncertainties in our estimates of biospheric Fm from field measurements (Figure 5a). Rivers with small catchment areas tend to have high Fm values while rivers with larger catchments show a wider range of Fm (Figure 5a). This behavior is predicted by our model wherein sufficient sediment storage is required to express differences in Fm values that result from variable POC cycling rates.

Our model predicts that variations in Fm for rivers with large catchment areas should depend on the rates of OC cycling, which we represent as the portion of slow POC. While it is difficult to independently quantify POC cycling rates at each of these sites, the observed meridional dependence of POC cycling implies that latitude can be used as a proxy for POC cycling rates (Carvalhais et al., 2014). Consistent with this, the larger catchments with high Fm values are all from low latitudes while the larger catchments with low Fm values are from high latitudes (Figure 5a).

Our model predictions of the relationship between catchment area and Fm are sensitive to both the portion of slow POC as well as T_{cut} (Figure 5a). In an attempt to control for the dependence of T_{cut} on the relationships shown in Figure 5a, we compare Fm values with the relative transit time metric developed in Section 3.1.1 (Equation 16), which accounts for predicted differences in T_{cut} using variations in w^3/Q_s. Comparing the relative transit time of each river with the biospheric Fm yields a relationship consistent with our model predictions (Figure 5b). As the relative transit time increases, biospheric Fm decreases as a result of radioactive decay during storage (Figure 5b). As expected, the exact relationship between relative transit time and biospheric Fm is variable between sites due to the effects of OC cycling (Figure 5b). By analyzing relative transit times (Figure 5b), we showed that the observed variations in the Fm of riverine biospheric POC are not solely due to variations in OC cycling, but also arise from variations in sediment storage.

Earth Surf. Dynam. Discuss., doi:10.5194/esurf-2017-29, 2017
Manuscript under review for journal Earth Surf. Dynam.
Discussion started: 15 May 2017

Earth Surface Dynamics Discussions
Open Access
EGU

570 **4 Discussion**

4.1 Behavior of biogeochemical cycles

The storage of aged POC predicted by our model has implications for global biogeochemical cycles. Observations (Torn et al., 1997; Lawrence et al., 2015) and basic OC cycling models (e.g., Jenny et al., 1949) link the age of a soil or sediment deposit to its radiocarbon content and OC inventory. 575 At the scale of river catchments, the amount of time available for OC accumulation and radioactive decay is set by the patterns of channel migration with time. These patterns lead to the preferential erosion of young deposits (Figure 3a). Consequently, old deposits, which have accumulated more OC, are preferentially retained in floodplains (Figure 3a). Thus, the dynamics of lateral channel migration imply that river deposits are a more sophisticated reservoir of OC than would be assumed 580 by the *null* hypothesis of a well-mixed system due to their age structure. Similarly, river dynamics also influence the expression of these storage processes in geochemical tracers (e.g., Fm) by setting the relative proportions of variably-aged river deposits sampled by fluvial erosion (Figure 3).

Typically, the low radiocarbon content of riverine POC is assumed to result from the erosion of petrogenic OC from sedimentary rocks (Masiello and Druffel, 2001; Bouchez et al., 2010; Galy 585 et al., 2008; Tao et al., 2015). Our results suggest that biospheric POC stored in river deposits can be another source of riverine POC that is depleted in radiocarbon. While our model predicts the bulk Fm of this stored OC reservoir, this value is associated with the time-averaged behavior of the river system and represents the average of all POC eroded by channel migration. On short timescales, the Fm of biospheric POC sampled by fluvial erosion may deviate from the time-averaged value 590 predicted by our model depending on the ages of fluvial deposits being eroded. Potentially, such short term variations in the Fm of the biospheric end-member may account for the fact many of the rivers in our compilation do not conform to two-component mixing between petrogenic and biospheric POC (Section 2.5).

Many previous studies of the terrestrial OC cycle have focused on the transport of terrestrial OC 595 to marine depo-centers, where it can be buried and stored over geologic timescales (Galy et al., 2015; Hilton, 2016). While this is undoubtedly an important process, our calculations suggest that sediment storage times in river deposits may approach geologic timescales (e.g., up to 10^6 years; see also Pizzuto et al., 2016), and thus may play an important role in buffering changes in atmospheric CO_2 and O_2 concentrations. Moreover, the fluvial processes that dictate sediment storage 600 timescales will also influence how terrestrial OC is transfered to marine basins. As a result, linkages between tectonic/climatic forcings and OC burial fluxes should include the mechanics of the reservoirs associated with terrestrial sediment-routing systems.

Presently, our model only accounts for lateral movements of the river channel with time. In natural river systems, vertical changes driven by overbank deposition, subsidence, and aggradation may 605 also influence the age structure of riverine POC. Since most overbank deposition is focused near

Earth Surf. Dynam. Discuss., doi:10.5194/esurf-2017-29, 2017
Manuscript under review for journal Earth Surf. Dynam.
Discussion started: 15 May 2017

the active channel (Pizutto, 1987; Marriott, 1992; Aalto et al., 2008), the spatio-temporal pattern of lateral channel migration likely approximates the storage durations associated with these deposits. Overbank deposition distal to the channel coupled with subsidence can lead to the burial of sediment deposits below the scour depth of the migrating channel. By selectively removing the oldest deposits, this additional sediment (and POC) sink can truncate the distribution of sediment ages. Assuming a constant floodplain elevation, the time to bury a deposit beneath the scour depth can be approximated as the ratio of the channel depth to the subsidence rate. As long as this burial timescale is long relative to the upper bound of the storage duration distribution (β; Equation 14), then subsidence will play a subordinate role in setting the age distributions of riverine sediments and POC. This approach of comparing the timescales associated with lateral migration and sediment burial can be used to evaluate whether the model presented here is appropriate for a particular field system.

All together, the results of this study imply that the controls on the terrestrial OC cycle are not limited to the factors that affect rates of primary productivity and respiration, but also include the dynamics of terrestrial sedimentary systems (see also: Stallard, 1998; Galy et al., 2015; Hilton, 2016). Sediment transport processes dictate the time and space scales over which OC cycling occurs, warranting their explicit consideration in models of global biogeochemical cycles. Since the terrestrial biosphere, in turn, influences the behavior of fluvial systems (Tal and Paola, 2007; Gibling and Davies, 2012), there is scope for feedbacks between biogeochemistry, sediment transport processes, and the architecture of fluvial processes to have changed over Earth's history (Algeo and Scheckler, 1998; Gibling and Davies, 2012).

4.2 Interpretation of time-varying environmental signals

In addition to affecting the behavior of biogeochemical cycles, our predicted age distributions also have implications for how we interpret environmental changes preserved in sedimentary archives. For example, compound-specific isotopic analyses of terrestrial biomarkers are widely employed as proxies for environmental conditions (Eglinton and Eglinton, 2008). In systems where these compounds are delivered to a basin via an alluvial river system, they are likely to inherit some age structure as a result of sediment storage. This mixing of variably-aged biomarkers will act as a signal filter and modify the sedimentary expression of environmental changes preserved in the isotopic composition of these compounds (Douglas et al., 2014). While such "shredding" of environmental signals has been extensively considered for sediments (Jerolmack and Paola, 2010; Ganti et al., 2014; Pizzuto et al., 2016), here, we extended this type of analysis to organic biomarkers.

To explore the implications of our model predictions for the time-series analysis of terrestrial biomarkers, we convolved each simulated sediment transit time distribution with a known periodic signal to investigate the extent of amplitude damping and phase lag at different frequencies. We specifically looked at the sediment transit time distribution (Figure 3), and not the POC age distribution, to determine the maximum effect of sedimentary averaging on the modulation of environmental

Earth Surf. Dynam. Discuss., doi:10.5194/esurf-2017-29, 2017
Manuscript under review for journal Earth Surf. Dynam.
Discussion started: 15 May 2017

signals. This might also be more appropriate for biomarker studies, which often target recalcitrant compounds that resist degradation (Eglinton and Eglinton, 2008). By treating the problem in this manner, we made the limiting assumption that biomarkers are not continually produced during sediment transit (c.f. Ponton et al., 2014). As such, the results can be viewed as reflecting how the expression of a signal recorded in biomarkers sourced from an upland region is modulated by episodic downstream transport.

Our results show that low frequency (i.e., forcing period $>>$ mean transit time) environmental signals are likely to be robustly recorded in the isotopic composition of terrestrial biomarkers (Figure 6). However, higher frequency variability shows complex phasing and significant amplitude damping (Figure 6). In part, the large phase lags are due to our limiting assumption that biomarkers are not continually produced during sediment transit. Consequently, the time for a signal generated upstream to advect downstream increases with the number of transport events. As an end-member case, we can consider a scenario where the upland-sourced biomarkers are mixed with an *in situ* floodplain source that records environmental signals approximately in phase. In this case, the large phase lag between the two biomarker pools will cause destructive interference in the sedimentary expression of the environmental signal.

As we considered only a single end-member case here, we acknowledge that broad application of our model framework will likely require the explicit modeling of the production and consumption of organic biomarkers during fluvial transit (Galy et al., 2011; Ponton et al., 2014). Nevertheless, our main point is that knowledge of both the sediment transit time and POC age distributions may aid in the interpretation of proxy systems affected by fluvial averaging. Conversely, if the magnitude of the expected environmental signal was known independently, then its expression within a biomarker record could be used to infer properties of POC age distribution, as is done for water transit through catchment systems (e.g., McGuire and McDonnell, 2006; Kirchner, 2015). While this general approach was attempted by Douglas et al. (2014) using time-series of biomarkers in lake sediments, they assumed an arbitrary shape for the distribution of POC ages (a bimodal Gaussian distribution). Consequently, our modeling approach can be used to improve such efforts by providing a framework for generating more mechanistic POC age distributions.

5 Conclusions

Using simplified models that capture the physical processes associated with sediment storage for meandering rivers, we found that sediment transit times distributions have power-law behavior, though geometric constraints temper or limit the distribution. Coupling our model for sediment transit time distributions to a simple model of OC cycling yields a full model for the radiocarbon content of riverine POC that can help interpret field observations. Thus we have to consider sediment storage a major aspect of biogeochemical cycling that introduces a time continuum that runs from annual to

Earth Surf. Dynam. Discuss., doi:10.5194/esurf-2017-29, 2017
Manuscript under review for journal Earth Surf. Dynam.
Discussion started: 15 May 2017

potentially million-year timescales. A basic inference from the results of this study is that biomarkers will exhibit a delay and/or mixed signal that convolves both the forcing and the storage. Though complicating the interpretation of sedimentary records, this river-floodplain exchange behavior presents an opportunity to understand the timescales over which CO_2 is stored as organic matter in surface deposits.

6 Data Availability

The raw data utilized in the study were compiled from previously published works and are available in the cited manuscripts. In Table 2, we provide results derived from the data compilation. A working example of our sediment and carbon storage model is included as supplementary MATLAB script.

Acknowledgements. M.A.T. acknowledges support from a Caltech Texaco postdoctoral research fellowship, the California Alliance for the Graduate and Professoriate, and the Caltech Discovery Fund. All authors acknowledge the participants of the GE126 course at Caltech (co-taught by W.W.F, M.P.L., and A.J.W.) for providing some of the early ideas that led to this work. Helpful criticism of a draft version of this manuscript was supplied by Dr. Joel Schiengross.

[Figure 1 about here.]

[Figure 2 about here.]

[Figure 3 about here.]

[Figure 4 about here.]

[Figure 5 about here.]

[Figure 6 about here.]

[Table 1 about here.]

[Table 2 about here.]

References

Aalto, R., Lauer, J. W., and Dietrich, W. E.: Spatial and temporal dynamics of sediment accumulation and exchange along Strickland River floodplains (Papua New Guinea) over decadal-to-centennial timescales, Journal of Geophysical Research, 113, F01S04, doi:10.1029/2006JF000627, http://doi.wiley.com/10.1029/2006JF000627, 2008.

Adams, J. L., Tipping, E., Bryant, C. L., Helliwell, R. C., Toberman, H., and Quinton, J.: Aged riverine particulate organic carbon in four UK catchments, Science of The Total Environment, 536, 648–654, doi:10.1016/j.scitotenv.2015.06.141, http://linkinghub.elsevier.com/retrieve/pii/S0048969715303387, 2015.

Algeo, T. and Scheckler, S.: Terrestrial-marine teleconnections in the Devonian: links between the evolution of land plants, weathering processes, and marine anoxic events, Philosophical Transactions of the Royal Society B: . . . , pp. 113–130, http://www.ncbi.nlm.nih.gov/pmc/articles/PMC1692181/, 1998.

Alin, S. R., Aalto, R., Goni, M. a., Richey, J. E., and Dietrich, W. E.: Biogeochemical characterization of carbon sources in the Strickland and Fly rivers, Papua New Guinea, Journal of Geophysical Research: Earth Surface, 113, 1–21, doi:10.1029/2006JF000625, 2008.

Berner, R. A.: A rate model for organic matter decomposition during bacterial sulfate reduction in marine sediments, in: Colloq. Int. CNRS, vol. 293, pp. 35–44, 1980.

Berner, R. A.: Biogeochemical cycles of carbon and sulfur and their effect on atmospheric oxygen over phanerozoic time, Palaeogeography, Palaeoclimatology, Palaeoecology, 75, 97–122, doi:10.1016/0921-8181(89)90018-0, 1989.

Bird, M., Lloyd, J., and Farquhar, G.: Terrestrial carbon storage during the LGM, Nature, 371, 566, doi:10.1038/371566a0, 1994.

Black, E., Renshaw, C. E., Magilligan, F. J., Kaste, J. M., Dade, W. B., and Landis, J. D.: Determining lateral migration rates of meandering rivers using fallout radionuclides, Geomorphology, 123, 364–369, doi:10.1016/j.geomorph.2010.08.004, http://dx.doi.org/10.1016/j.geomorph.2010.08.004, 2010.

Blair, N. E. and Aller, R. C.: The fate of terrestrial organic carbon in the marine environment., Annual review of marine science, 4, 401–23, doi:10.1146/annurev-marine-120709-142717, 2012.

Blöthe, J. H. and Korup, O.: Millennial lag times in the Himalayan sediment routing system, Earth and Planetary Science Letters, 382, 38–46, doi:10.1016/j.epsl.2013.08.044, http://dx.doi.org/10.1016/j.epsl.2013.08.044, 2013.

Bolin, B. and Rodhe, H.: A note on the concepts of age distribution and transit time in natural reservoirs, Tellus A, 1, doi:10.3402/tellusa.v25i1.9644, 1973.

Bouchez, J., Beyssac, O., and Galy, V.: Oxidation of petrogenic organic carbon in the Amazon floodplain as a source of atmospheric CO2, Geology, 38, 255–258, doi:10.1130/G30608.1, 2010.

Bouchez, J., Galy, V., Hilton, R. G., Gaillardet, J., Moreira-Turcq, P., Pérez, M. A., France-Lanord, C., and Maurice, L.: Source, transport and fluxes of Amazon River particulate organic carbon: Insights from river sediment depth-profiles, Geochimica et Cosmochimica Acta, 133, 280–298, doi:10.1016/j.gca.2014.02.032, 2014.

Boudreau, B. P. and Ruddick, B. R.: On a reactive continuum representation of organic matter diagenesis, doi:10.2475/ajs.292.1.79, 1991.

Bradley, D. N. and Tucker, G. E.: The storage time, age, and erosion hazard of laterally accreted sediment on the floodplain of a simulated meandering river, Journal of Geophysical Research: Earth Surface, 118, 1308–1319, doi:10.1002/jgrf.20083, 2013.

Cartea, A. and Del-Castillo-Negrete, D.: Fluid limit of the continuous-time random walk with general Levy jump distribution functions, Physical Review E - Statistical, Nonlinear, and Soft Matter Physics, 76, 1–8, doi:10.1103/PhysRevE.76.041105, 2007.

Carvalhais, N., Forkel, M., Khomik, M., Bellarby, J., Jung, M., Migliavacca, M., Mingquan, M., Saatchi, S., Santoro, M., Thurner, M., Weber, U., Ahrens, B., Beer, C., Cescatti, A., Randerson, J. T., and Reichstein, M.: Global covariation of carbon turnover times with climate in terrestrial ecosystems, Nature, 514, 213–217, doi:10.1038/nature13731, http://dx.doi.org/10.1038/nature13731, 2014.

Cathalot, C., Rabouille, C., Tisnérat-Laborde, N., Toussaint, F., Kerhervé, P., Buscail, R., Loftis, K., Sun, M. Y., Tronczynski, J., Azoury, S., Lansard, B., Treignier, C., Pastor, L., and Tesi, T.: The fate of river organic carbon in coastal areas: A study in the Rhone River delta using multiple isotopic (δ13C, δ14C) and organic tracers, Geochimica et Cosmochimica Acta, 118, 33–55, doi:10.1016/j.gca.2013.05.001, 2013.

Clark, K. E., Hilton, R. G., West, A. J., Malhi, Y., Gröcke, D. R., Bryant, C. L., Ascough, P. L., Robles Caceres, A., and New, M.: New views on "old" carbon in the Amazon River: Insight from the source of organic carbon eroded from the Peruvian Andes, Geochemistry, Geophysics, Geosystems, 14, 1644–1659, doi:10.1002/ggge.20122, 2013.

Constantine, J. A., Dunne, T., Ahmed, J., Legleiter, C., and Eli, D.: Sediment supply as a driver of river evolution in the Amazon Basin, Nature Geoscience, 7, 899–903, doi:10.1038/NGEO2282, 2014.

Dosseto, a., Bourdon, B., Gaillardet, J., Allegre, C., and Filizola, N.: Time scale and conditions of weathering under tropical climate: Study of the Amazon basin with U-series, Geochimica et Cosmochimica Acta, 70, 71–89, doi:10.1016/j.gca.2005.06.033, 2006.

Douglas, P. M. J., Pagani, M., Eglinton, T. I., Brenner, M., Hodell, D. A., Curtis, J. H., Ma, K. F., and Breckenridge, A.: Pre-aged plant waxes in tropical lake sediments and their influence on the chronology of molecular paleoclimate proxy records, Geochimica et Cosmochimica Acta, 141, 346–364, doi:10.1016/j.gca.2014.06.030, http://dx.doi.org/10.1016/j.gca.2014.06.030, 2014.

Dunne, T. and Aalto, R. E.: Large River Floodplains, vol. 9, doi:10.1016/B978-0-12-374739-6.00258-X, http://dx.doi.org/10.1016/B978-0-12-374739-6.00258-X, 2013.

Eglinton, T. I. and Eglinton, G.: Molecular proxies for paleoclimatology, Earth and Planetary Science Letters, 275, 1–16, doi:10.1016/j.epsl.2008.07.012, 2008.

Feng, X., Benitez-Nelson, B. C., Montluçon, D. B., Prahl, F. G., McNichol, A. P., Xu, L., Repeta, D. J., and Eglinton, T. I.: 14C and 13C characteristics of higher plant biomarkers in Washington margin surface sediments, Geochimica et Cosmochimica Acta, 105, 14–30, doi:10.1016/j.gca.2012.11.034, 2013.

Fischlin, A., Midgley, G., Price, J., Leemans, R., Gopal, B., Turley, C., Rounsevell, M., Dube, O., Tarazona, J., and Velichko, A.: Ecosystems, their properties, goods and services, in: Climate Change 2007: Impacts, Adaptation and Vulnerability. Contribution of Working Group II to the Fourth Assessment Report of the Intergovernmental Panel of Climate Change, chap. 4, pp. 211–272, Cambridge University Press, doi:http://www.gtp89.dial.pipex.com/04.pdf, 2007.

France-Lanord, C. and Derry, L. A.: Organic carbon burial forcing of the carbon cycle from Himalayan erosion, Nature, 390, 65–67, doi:10.1038/36324, 1997.

Frascati, A. and Lanzoni, S.: Morphodynamic regime and long-term evolution of meandering rivers, Journal of Geophysical Research: Earth Surface, 114, 1–12, doi:10.1029/2008JF001101, 2009.

Galy, V. and Eglinton, T.: Protracted storage of biospheric carbon in the Ganges–Brahmaputra basin, Nature Geoscience, 4, 843–847, doi:10.1038/ngeo1293, 2011.

Galy, V., France-Lanord, C., Beyssac, O., Faure, P., Kudrass, H., and Palhol, F.: Efficient organic carbon burial in the Bengal fan sustained by the Himalayan erosional system., Nature, 450, 407–10, doi:10.1038/nature06273, http://www.ncbi.nlm.nih.gov/pubmed/18004382, 2007.

Galy, V., Beyssac, O., France-Lanord, C., and Eglinton, T.: Recycling of graphite during Himalayan erosion: a geological stabilization of carbon in the crust., Science (New York, N.Y.), 322, 943–5, doi:10.1126/science.1161408, http://www.ncbi.nlm.nih.gov/pubmed/18988852, 2008.

Galy, V., Eglinton, T., France-Lanord, C., and Sylva, S.: The provenance of vegetation and environmental signatures encoded in vascular plant biomarkers carried by the Ganges-Brahmaputra rivers, Earth and Planetary Science Letters, 304, 1–12, doi:10.1016/j.epsl.2011.02.003, 2011.

Galy, V., Peucker-Ehrenbrink, B., and Eglinton, T.: Global carbon export from the terrestrial biosphere controlled by erosion, Nature, 521, 204–207, doi:10.1038/nature14400, 2015.

Ganti, V., Straub, K. M., Foufoula-Georgiou, E., and Paola, C.: Space-time dynamics of depositional systems: Experimental evidence and theoretical modeling of heavy-tailed statistics, Journal of Geophysical Research: Earth Surface, 116, 1–17, doi:10.1029/2010JF001893, 2011.

Ganti, V., Lamb, M. P., and McElroy, B.: Quantitative bounds on morphodynamics and implications for reading the sedimentary record, Nature communications, 5, 3298, doi:10.1038/ncomms4298, http://www.ncbi.nlm.nih.gov/pubmed/24576990, 2014.

Gao, Q., Tao, Z., Guanrong, Y., Ding, J., Liu, Z., and Liu, K.: Elemental and isotopic signatures of particulate organic carbon in the Zengjiang River, southern China, Hydrological Processes, 21, 1318–1327, doi:10.1002/hyp, 2007.

Gibling, M. R. and Davies, N. S.: Palaeozoic landscapes shaped by plant evolution, Nature Geoscience, 5, 99–105, doi:10.1038/ngeo1376, http://dx.doi.org/10.1038/ngeo1376, 2012.

Goñi, M. A., Hatten, J. A., Wheatcroft, R. A., and Borgeld, J. C.: Particulate organic matter export by two contrasting small mountainous rivers from the Pacific Northwest, U.S.A., Journal of Geophysical Research: Biogeosciences, 118, 112–134, doi:10.1002/jgrg.20024, 2013.

Gordon, E. S. and Goni, M. a.: Sources and distribution of terrigenous organic matter delivered by the Atchafalaya River to sediments in the northern Gulf of Mexico, Geochimica et Cosmochimica Acta, 67, 2359–2375, doi:10.1016/S0016-7037(02)01412-6, 2003.

Granet, M., Chabaux, F., Stille, P., Dosseto, a., France-Lanord, C., and Blaes, E.: U-series disequilibria in suspended river sediments and implication for sediment transfer time in alluvial plains: The case of the Himalayan rivers, Geochimica et Cosmochimica Acta, 74, 2851–2865, doi:10.1016/j.gca.2010.02.016, http://dx.doi.org/10.1016/j.gca.2010.02.016http://linkinghub.elsevier.com/retrieve/pii/S0016703710000852, 2010.

Grenfell, M., Aalto, R., and Nicholas, A.: Chute channel dynamics in large, sand-bed meandering rivers, Earth Surface Processes and Landforms, 37, 315–331, doi:10.1002/esp.2257, http://dx.doi.org/10.1002/esp.2257, 2012.

Hack, J.: Studies of longitudinal stream profiles in Virginia and Maryland, USGS Professional Paper 249, p. 97, geomorph, 1957.

Hatten, J. a., Goñi, M. a., and Wheatcroft, R. a.: Chemical characteristics of particulate organic matter from a small, mountainous river system in the Oregon Coast Range, USA, Biogeochemistry, 107, 43–66, doi:10.1007/s10533-010-9529-z, 2012.

Hickin, E. J. and Nanson, G. C.: The character of channel migration on the Beatton River, Northeast British Columbia, Canada, Bulletin of the Geological Society of America, 86, 487–494, doi:10.1130/0016-7606(1975)86<487:TCOCMO>2.0.CO;2, 1975.

Hilton, R. G.: Climate regulates the erosional carbon export from the terrestrial biosphere, Geomorphology, doi:10.1016/j.geomorph.2016.03.028, http://dx.doi.org/10.1016/j.geomorph.2016.03.028, 2016.

Hilton, R. G., Galy, A., Hovius, N., Horng, M.-J., and Chen, H.: The isotopic composition of particulate organic carbon in mountain rivers of Taiwan, Geochimica et Cosmochimica Acta, 74, 3164–3181, doi:10.1016/j.gca.2010.03.004, http://linkinghub.elsevier.com/retrieve/pii/S0016703710001183, 2010.

Hilton, R. G., Galy, V., Gaillardet, J., Dellinger, M., Bryant, C., O'Regan, M., Gröcke, D. R., Coxall, H., Bouchez, J., and Calmels, D.: Erosion of organic carbon in the Arctic as a geological carbon dioxide sink, Nature, 524, 84–87, doi:10.1038/nature14653, http://www.nature.com/doifinder/10.1038/nature14653, 2015.

Howard, A. D. and Knutson, T. R.: Sufficient conditions for river meandering: A simulation approach, doi:10.1029/WR020i011p01659, 1984.

Hu, B., Li, J., Bi, N., Wang, H., Wei, H., Zhao, J., Xie, L., Zou, L., Cui, R., Li, S., Liu, M., and Li, G.: Effect of human-controlled hydrological regime on the source, transport, and flux of particulate organic carbon from the lower Huanghe (Yellow River), Earth Surface Processes and Landforms, 1042, n/a–n/a, doi:10.1002/esp.3702, http://doi.wiley.com/10.1002/esp.3702, 2015.

Jenny, H., Gessel, S. P., and Bingham, F. T.: Comparative study of decomposition rates of organic matter in temperate and tropical regions., Soil Science, 68, 419–432, 1949.

Jerolmack, D. J. and Paola, C.: Shredding of environmental signals by sediment transport, Geophysical Research Letters, 37, 1–5, doi:10.1029/2010GL044638, 2010.

Jørgensen, B.: A comparison of methods for the quantification of bacterial sulfate reduction in coastal marine sediments, 1978.

Kao, S.-J. and Liu, K.-K.: Particulate organic carbon export from a subtropical mountainous river (Lanyang Hsi) in Taiwan, Limnology and Oceanography, 41, 1749–1757, doi:10.4319/lo.1996.41.8.1749, 1996.

Katsev, S. and Crowe, S. a.: Organic carbon burial efficiencies in sediments: The power law of mineralization revisited, Geology, 43, 607–610, doi:10.1130/G36626.1, 2015.

Keeling, C. D.: The Concentration and Isotopic Abundances of Carbon Dioxide in the Atmosphere, Tellus, 12, 200–203, doi:10.1111/j.2153-3490.1960.tb01300.x, 1960.

Keeling, R. F. and Shertz, S. R.: Seasonal and interannual variations in atmospheric oxygen and implications for the global carbon cycle, Nature, 358, 723–727, doi:10.1038/358723a0, 1992.

Kirchner, J. W.: Aggregation in environmental systems: seasonal tracer cycles quantify young water fractions, but not mean transit times, in spatially heterogeneous catchments, Hydrology and Earth System Sciences Discussions, 12, 3059–3103, doi:10.5194/hessd-12-3059-2015, 2015.

Komada, T., Druffel, E. R. M., and Trumbore, S. E.: Oceanic export of relict carbon by small mountainous rivers, Geophysical Research Letters, 31, doi:10.1029/2004GL019512, 2004.

Lancaster, S. T. and Bras, R. L.: A simple model of river meandering and its comparison to natural channels, Hydrological Processes, 16, 1–26, doi:10.1002/hyp.273, 2002.

Lancaster, S. T. and Casebeer, N. E.: Sediment storage and evacuation in headwater valleys at the transition between debris-flow and fluvial processes, Geology, 35, 1027–1030, doi:10.1130/G239365A.1, 2007.

Lauer, J. W. and Parker, G.: Modeling framework for sediment deposition, storage, and evacuation in the floodplain of a meandering river: Theory, Water Resources Research, 44, n/a–n/a, doi:10.1029/2006WR005528, 2008a.

Lauer, J. W. and Parker, G.: Net local removal of floodplain sediment by river meander migration, Geomorphology, 96, 123–149, doi:10.1016/j.geomorph.2007.08.003, 2008b.

Lauer, J. W. and Willenbring, J.: Steady state reach-scale theory for radioactive tracer concentration in a simple channel/floodplain system, Journal of Geophysical Research, 115, F04 018, doi:10.1029/2009JF001480, http://doi.wiley.com/10.1029/2009JF001480, 2010.

Lawrence, C. R., Harden, J. W., Xu, X., Schulz, M. S., and Trumbore, S. E.: Long-term controls on soil organic carbon with depth and time: A case study from the Cowlitz River Chronosequence, WA USA, Geoderma, 247-248, 73–87, doi:10.1016/j.geoderma.2015.02.005, http://dx.doi.org/10.1016/j.geoderma.2015.02.005, 2015.

Leithold, E. L., Blair, N. E., and Perkey, D. W.: Geomorphologic controls on the age of particulate organic carbon from small mountainous and upland rivers, Global Biogeochemical Cycles, 20, GB3022, doi:10.1029/2005GB002677, 2006.

Li, C., Yang, S., Zhao, J. x., Dosseto, A., Bi, L., and Clark, T. R.: The time scale of river sediment source-to-sink processes in East Asia, Chemical Geology, 446, 138–146, doi:10.1016/j.chemgeo.2016.06.012, http://dx.doi.org/10.1016/j.chemgeo.2016.06.012, 2016.

Li, G., Wang, X. T., Yang, Z., Mao, C., West, a. J., and Ji, J.: Dam-triggered organic carbon sequestration makes the Changjiang (Yangtze) river basin (China) a significant carbon sink, Journal of Geophysical Research G: Biogeosciences, 120, 39–53, doi:10.1002/2014JG002646, 2015.

Limaye, A. B. S. and Lamb, M. P.: A vector-based method for bank-material tracking in coupled models of meandering and landscape evolution, Journal of Geophysical Research-Earth Surface, 118, 2421–2437, doi:Doi 10.1002/2013jf002854, 2013.

Malmon, D. V., Dunne, T., Reneau, S. L., The, S., and September, N.: Stochastic Theory of Particle Trajectories through Alluvial Valley Floors, The Journal of Geology, 111, 525–542, doi:10.1086/376764, 2003.

Mantegna, R. N. and Stanley, H. E.: Stochastic process with ultrasound convergence to a Gaussian : truncated Levy flight, Phys. Rev. Lett., 73, 2946, doi:10.1103/PhysRevLett.73.2946, 1994.

Marriott, S.: Textural analysis and modelling of a flood deposit: River Severn, UK, Earth Surface Processes and Landforms, 17, 687–697, 1992.

Martin, E. E., Ingalls, A. E., Richey, J. E., Keil, R. G., Santos, G. M., Truxal, L. T., Alin, S. R., and Druffel, E. R. M.: Age of riverine carbon suggests rapid export of terrestrial primary production in tropics, Geophysical Research Letters, 40, 5687–5691, doi:10.1002/2013GL057450, 2013.

Masiello, C. A. and Druffel, E. R. M.: Carbon Isotope Geochemistry of the Santa Clara River, Global Biogeochemical Cycles, 15, 407–416, http://cat.inist.fr/?aModele=afficheN&cpsidt=1038975, 2001.

Masiello, C. A., Chadwick, O. A., Southon, J., Torn, M. S., and Harden, J. W.: Weathering controls on mechanisms of carbon storage in grassland soils, Global Biogeochemical Cycles, 18, 1–9, doi:10.1029/2004GB002219, 2004.

McGuire, K. J. and McDonnell, J. J.: A review and evaluation of catchment transit time modeling, Journal of Hydrology, 330, 543–563, doi:10.1016/j.jhydrol.2006.04.020, 2006.

Meerschaert, M. M., Roy, P., and Shao, Q.: Parameter estimation for exponentially tempered power law distributions, Communications in Statistics-Theory and Methods, 41, 1839–1856, doi:10.1080/03610926.2011.552828, 2010.

Middelburg, J. J.: A simple rate model for organic matter decomposition in marine sediments, Geochimica et Cosmochimica Acta, 53, 1577–1581, doi:10.1016/0016-7037(89)90239-1, 1989.

Mueller, J. E.: Re-evaluation of the relationship of master streams and drainage basins: Reply, Geol. Soc. Am. Bull, 84, 3127–3130, doi:10.1130/0016-7606(1973)84<3127:ROTROM>2.0.CO;2, 1973.

Nagao, S., Usui, T., Yamamoto, M., Minagawa, M., Iwatsuki, T., and Noda, A.: Combined use of D14C and d13C values to trace transportation and deposition processes of terrestrial particulate organic matter in coastal marine environments, Chemical Geology, 218, 63–72, doi:10.1016/j.chemgeo.2005.01.025, 2005.

Nakamura, F. and Kikuchi, S.-i.: Transport Processes Using Age Distribution of Floodplain Deposits, Geomorphology, 16, 139–145, 1996.

Nitsche, M., Rickenmann, D., Kirchner, J. W., Turowski, J. M., and Badoux, A.: Macroroughness and variations in reach-averaged flow resistance in steep mountain streams, Water Resources Research, 48, 1–16, doi:10.1029/2012WR012091, 2012.

Pizutto, J. E.: Sediment diffusion during overbank flows, Sedimentology, 34, 301–317, doi:10.1111/j.1365-3091.1987.tb00779.x, 1987.

Pizzuto, J., Schenk, E. R., Hupp, C. R., Gellis, A., Noe, G., Williamson, E., Karwan, D. L., O'Neal, M., Marquard, J., Aalto, R., and Newbold, D.: Characteristic length scales and time-averaged transport velocities of suspended sediment in the mid-Atlantic Region, USA, Water Resources Research, 50, 790–805, doi:10.1002/2013WR014485, 2014.

Pizzuto, J., Keeler, J., Skalak, K., and Karwan, D.: Storage filters upland suspended sediment signals delivered from watersheds, Geology, 44, G38 170.1, doi:10.1130/G38170.1, http://geology.gsapubs.org/lookup/doi/10.1130/G38170.1, 2016.

Ponton, C., West, A. J., Feakins, S. J., and Galy, V.: Leaf wax biomarkers in transit record river catchment composition, Geophysical Research Letters, 41, 6420–6427, doi:10.1002/2014GL061328.Received, 2014.

Rosenheim, B. E., Roe, K. M., Roberts, B. J., Kolker, A. S., Allison, M. a., and Johannesson, K. H.: River discharge influences on particulate organic carbon age structure in the Mississippi/Atchafalaya River System, Global Biogeochemical Cycles, 27, 154–166, doi:10.1002/gbc.20018, 2013.

Rosiński, J.: Tempering stable processes, Stochastic Processes and their Applications, 117, 677–707, doi:10.1016/j.spa.2006.10.003, 2007.

Sadler, P. M.: Sediment accumulation rates and the completeness of stratigraphic sections, The Journal of Geology, 89, 569–584, 1981.

Schefuß, E., Eglinton, T. I., Spencer-Jones, C. L., Rullkötter, J., De Pol-Holz, R., Talbot, H. M., Grootes, P. M., and Schneider, R. R.: Hydrologic control of carbon cycling and aged carbon discharge in the Congo River basin, Nature Geoscience, 9, doi:10.1038/ngeo2778, http://www.nature.com/doifinder/10.1038/ngeo2778, 2016.

Schmidt, M. W. I., Torn, M. S., Abiven, S., Dittmar, T., Guggenberger, G., Janssens, I. a., Kleber, M., Kögel-Knabner, I., Lehmann, J., Manning, D. a. C., Nannipieri, P., Rasse, D. P., Weiner, S., and Trumbore, S. E.: Persistence of soil organic matter as an ecosystem property, Nature, 478, 49–56, doi:10.1038/nature10386, 2011.

Schwenk, J., Lanzoni, S., and Foufoula-Georgiou, E.: The life of a meander bend: Connecting shape and dynamics via analysis of a numerical model, Journal of Geophysical Research F: Earth Surface, 120, 690–710, doi:10.1002/2014JF003252, 2015.

Smith, J. C., Galy, A., Hovius, N., Tye, A. M., Turowski, J. M., and Schleppi, P.: Runoff-driven export of particulate organic carbon from soil in temperate forested uplands, Earth and Planetary Science Letters, 365, 198–208, doi:10.1016/j.epsl.2013.01.027, http://dx.doi.org/10.1016/j.epsl.2013.01.027, 2013.

Stallard, R. F.: Terrestrial sedimentation and the carbon cycle: Coupling weathering and erosion to carbon burial, Global Biogeochemical Cycles, 12, 231–257, doi:10.1029/98GB00741, 1998.

Tal, M. and Paola, C.: Dynamic single-thread channels maintained by the interaction of flow and vegetation, Geology, 35, 347–350, doi:10.1130/G23260A.1, 2007.

Tao, S., Eglinton, T. I., Montluçon, D. B., McIntyre, C., and Zhao, M.: Pre-aged soil organic carbon as a major component of the Yellow River suspended load: Regional significance and global relevance, Earth and Planetary Science Letters, 414, 77–86, doi:10.1016/j.epsl.2015.01.004, http://www.sciencedirect.com/science/article/pii/S0012821X15000175, 2015.

Torn, M. S., Trumbore, S. E., Chadwick, O. a., Vitousek, P. M., and Hendricks, D. M.: Mineral control of soil organic carbon storage and turnover, Nature, 389, 3601–3603, doi:10.1038/38260, 1997.

Townsend-Small, A., Noguera, J. L., McClain, M. E., and Brandes, J. a.: Radiocarbon and stable isotope geochemistry of organic matter in the Amazon headwaters, Peruvian Andes, Global Biogeochemical Cycles, 21, 1–9, doi:10.1029/2006GB002835, 2007.

Turowski, J. M., Hilton, R. G., and Sparkes, R.: Decadal carbon discharge by a mountain stream is dominated by coarse organic matter, Geology, 44, 27–30, doi:10.1130/G37192.1, 2016.

Voss, B. M.: Spatial and temporal dynamics of biogeochemical processes in the Fraser River, Canada: A coupled organic-inorganic perspective, Ph.D. thesis, WOODS HOLE OCEANOGRAPHIC INSTITUTION, 2014.

Wang, X., Ma, H., Li, R., Song, Z., and Wu, J.: Seasonal fluxes and source variation of organic carbon transported by two major Chinese Rivers: The Yellow River and Changjiang (Yangtze) River, Global Biogeochemical Cycles, 26, 1–10, doi:10.1029/2011GB004130, 2012.

Williams, G. P.: River Meanders and Channel Size, Journal of Hydrology, 88, 147–164, 1986.

Wittmann, H., Von Blanckenburg, F., Dannhaus, N., Bouchez, J., Gaillardet, J., Guyot, J. L., Maurice, L., Roig, H., Filizola, N., and Christl, M.: A test of the cosmogenic 10Be(meteoric)/9Be proxy for simultaneously determining basin-wide erosion rates, denudation rates, and the degree of weathering in the Amazon basin, Journal of Geophysical Research-Earth Surface, pp. 2498–2528, doi:10.1002/2015JF003581.Received, 2015.

Wittmann, H., Malusà, M. G., Resentini, A., Garzanti, E., and Niedermann, S.: The cosmogenic record of mountain erosion transmitted across a foreland basin: source-to-sink analysis of in situ 10Be, 26Al and 21Ne in sediment of the Po river catchment, Earth and Planetary Science Letters, 452, 258–271, doi:10.1016/j.epsl.2016.07.017, http://dx.doi.org/10.1016/j.epsl.2016.07.017, 2016.

Earth Surf. Dynam. Discuss., doi:10.5194/esurf-2017-29, 2017
Manuscript under review for journal Earth Surf. Dynam.
Discussion started: 15 May 2017

List of Figures

1 Model schematic highlighting key geometric relationships. The sediment flux (Q_s) from an upstream area is routed though an alluvial valley. As a result of lateral channel migration (E_L), sediment deposits are created and eroded leading to transient sediment storage. During sediment storage, the fixation of atmospheric CO_2 by biota leads to the production (P) of particulate organic carbon (C), which is degraded back to CO_2 at a rate (k) proportional to its concentration in sediments. At any time, the ages of sediments and organic carbon can be described by two distributions. The storage duration distribution describes the ages of material being actively removed from the system by erosion and thus have reached their maximum age. The deposit age distribution describes the ages of material that remains stored in river deposits and will continue to age until subsequent erosion. 32

2 Sediment transport parameters in the model and field data. (a) The results of the numerical meandering model simulations that show that the meander bend growth timescale (T_{cut}) is correlated with the time required for the channel to migrate one channel width at the maximum lateral migration rate ($E_{L,max}$). (b) Field evidence for a correlation between the mean time required to migrate one channel width (w/E_L) and the sediment supply timescale (w^3/Q_s). (c) Jitter plot of calculated x_{tran} values (Equation 4) for the field data shown in (b). Together, these panels show that T_{cut} scales with the lateral migration rate, which, in field data, is correlated with suspended sediment fluxes (Constantine et al., 2014). The correlation between lateral migration rates and sediment fluxes results in minimal variation in the transport length scale (c) and provides a proxy for T_{cut} (i.e., w^3/Q_s) for rivers where lateral migration rates are unknown. 33

3 Dimensionless age distributions. (a) The survival function (complementary cumulative distribution function) of sediment storage durations (red points) derived from the meandering model. The sediment storage durations are normalized by a cutoff time (T_{cut}) of 350 years based on explicit tracking of meander bend growth (Schwenk et al., 2015). The model results were fit to a tempered Pareto distribution and the best-fitting model is shown as a red line. Also shown is a tempered Pareto fit to the distribution of deposit ages at the end of the model simulation (black line). (b-c) The change in the shape of the sediment transit time distribution (normalized by T_{cut}; Equation 3) with increasing number of transport events. (b) The mean, median, and 90% confidence interval of the sediment transit time distributions for 1 to 20 transport events. (c) The probability density function of sediment transit time distributions for 1 and 20 transport events. Consistent with the central limit theorem, the shape of the sediment transit distribution varies with the number of transport events. 34

Earth Surf. Dynam. Discuss., doi:10.5194/esurf-2017-29, 2017
Manuscript under review for journal Earth Surf. Dynam.
Discussion started: 15 May 2017

4 Model predictions of the radiocarbon content of POC. (a) Predicted relationships between sediment mean transit times (MTTs) and the Fm of biospheric POC for POC cycling models with variable proportions of slow POC ($\%S$) and variable slow POC consumption rate constants (kS). The Fm values shown as shaded areas were calculated using sediment transit time distributions (TTDs) with shapes set by between 1 to 20 transport events (Figure 3) and MTTs between 10^3 and 10^6 years. The model results show that plausible sediment TTDs yield significantly different relationships between the MTT and Fm relative to predictions for systems with a single transit time (solid bold lines). While TTD shape is an important factor reflected in the vertical range of each shaded area, the model results suggest that large differences of OC cycling (different colors; see figure legend) are distinguishable in the relationships between the MTT and Fm. (b) Predicted downstream profiles of Fm for a fixed x_{tran} (100 km), but variable T_{cut} (100 and 1000 years) and POC cycling parameters (different line styles; see figure legend). The model results suggest that observed downstream profiles are sensitive to both sediment storage timescales, which are controlled by T_{cut}, as well as OC cycling parameters. 35

5 Field data compilation and comparison with model predictions. Field data are color coded based on their latitude as a proxy for POC cycling rates. (a) Model curves and field measurements of the relationship between catchment area and bulk biospheric Fm. Model curves are drawn for fixed POC consumption rate constants, but variable steady-state proportions of "slow" cycling POC and T_{cut} values (see legend). (b) Measured biospheric Fm values compared to our relative transit time metric (Equation 16), which is based on Hack's Law (Hack, 1957) and scaling relationships shown in Figures 2 and 3. The field data are consistent with the model predictions of aged POC in rivers with larger catchment areas and slower migration rates (inferred from variations in w^3/Q_s) and thus longer sediment storage times. We note that in our compilation of rivers with measurements of biospheric Fm, catchment area and w^3/Q_s are correlated. 36

6 Effect of floodplain storage on environmental signals recorded by organic biomarkers. This figure shows the effect of convolving our sediment transit time distributions with a sine wave where the period of the sinusoidal input is equal to the mean transit time (a), twice the mean transit time (b), five times the mean transit time (c), and 10 times the mean transit time (d). The amplitude and phase of the sinusoidal input is shown as the black dashed lines. The colored lines refer to the output signal with the color reflecting the number of transport events (see color bar), which sets the shape of the transit time distribution. The model results suggest that climate signals recorded in terrestrial biomarkers will be significantly modulated if their period is short relative to the mean sediment transit time. 37

Earth Surf. Dynam. Discuss., doi:10.5194/esurf-2017-29, 2017
Manuscript under review for journal Earth Surf. Dynam.
Discussion started: 15 May 2017

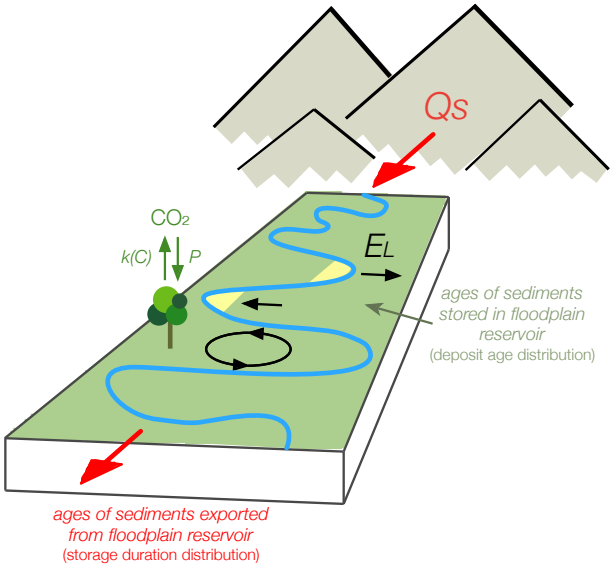

Figure 1. Model schematic highlighting key geometric relationships. The sediment flux (Q_s) from an upstream area is routed though an alluvial valley. As a result of lateral channel migration (E_L), sediment deposits are created and eroded leading to transient sediment storage. During sediment storage, the fixation of atmospheric CO_2 by biota leads to the production (P) of particulate organic carbon (C), which is degraded back to CO_2 at a rate (k) proportional to its concentration in sediments. At any time, the ages of sediments and organic carbon can be described by two distributions. The storage duration distribution describes the ages of material being actively removed from the system by erosion and thus have reached their maximum age. The deposit age distribution describes the ages of material that remains stored in river deposits and will continue to age until subsequent erosion.

Earth Surf. Dynam. Discuss., doi:10.5194/esurf-2017-29, 2017
Manuscript under review for journal Earth Surf. Dynam.
Discussion started: 15 May 2017

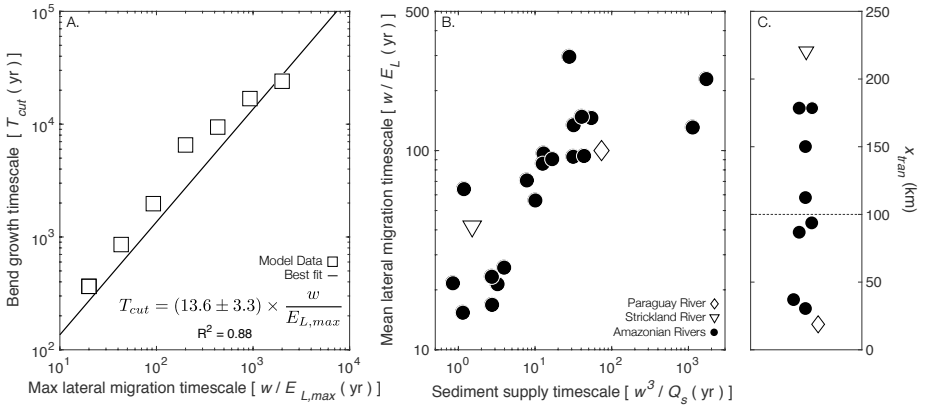

Figure 2. Sediment transport parameters in the model and field data. (a) The results of the numerical meandering model simulations that show that the meander bend growth timescale (T_{cut}) is correlated with the time required for the channel to migrate one channel width at the maximum lateral migration rate ($E_{L,max}$). (b) Field evidence for a correlation between the mean time required to migrate one channel width (w/E_L) and the sediment supply timescale (w^3/Q_s). (c) Jitter plot of calculated x_{tran} values (Equation 4) for the field data shown in (b). Together, these panels show that T_{cut} scales with the lateral migration rate, which, in field data, is correlated with suspended sediment fluxes (Constantine et al., 2014). The correlation between lateral migration rates and sediment fluxes results in minimal variation in the transport length scale (c) and provides a proxy for T_{cut} (i.e., w^3/Q_s) for rivers where lateral migration rates are unknown.

Earth Surf. Dynam. Discuss., doi:10.5194/esurf-2017-29, 2017
Manuscript under review for journal Earth Surf. Dynam.
Discussion started: 15 May 2017

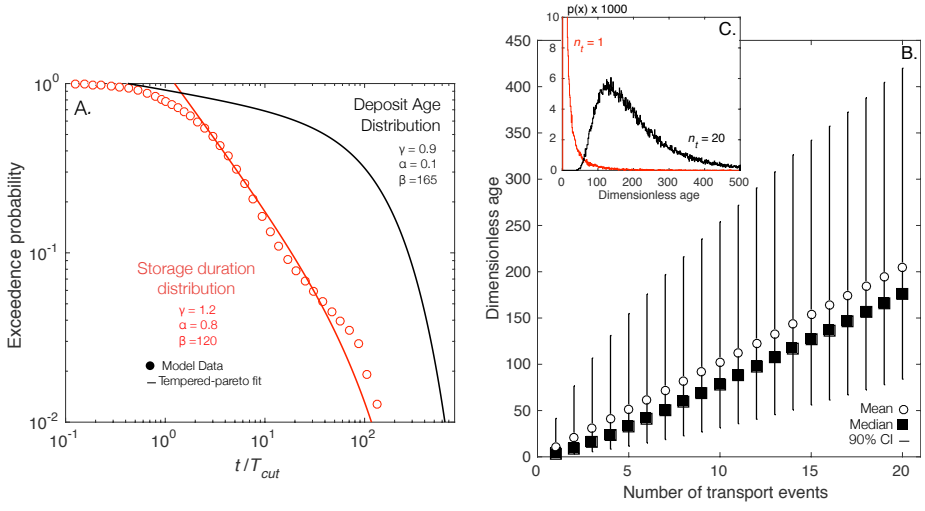

Figure 3. Dimensionless age distributions. (a) The survival function (complementary cumulative distribution function) of sediment storage durations (red points) derived from the meandering model. The sediment storage durations are normalized by a cutoff time (T_{cut}) of 350 years based on explicit tracking of meander bend growth (Schwenk et al., 2015). The model results were fit to a tempered Pareto distribution and the best-fitting model is shown as a red line. Also shown is a tempered Pareto fit to the distribution of deposit ages at the end of the model simulation (black line). (b-c) The change in the shape of the sediment transit time distribution (normalized by T_{cut}; Equation 3) with increasing number of transport events. (b) The mean, median, and 90% confidence interval of the sediment transit time distributions for 1 to 20 transport events. (c) The probability density function of sediment transit time distributions for 1 and 20 transport events. Consistent with the central limit theorem, the shape of the sediment transit distribution varies with the number of transport events.

Earth Surf. Dynam. Discuss., doi:10.5194/esurf-2017-29, 2017
Manuscript under review for journal Earth Surf. Dynam.
Discussion started: 15 May 2017

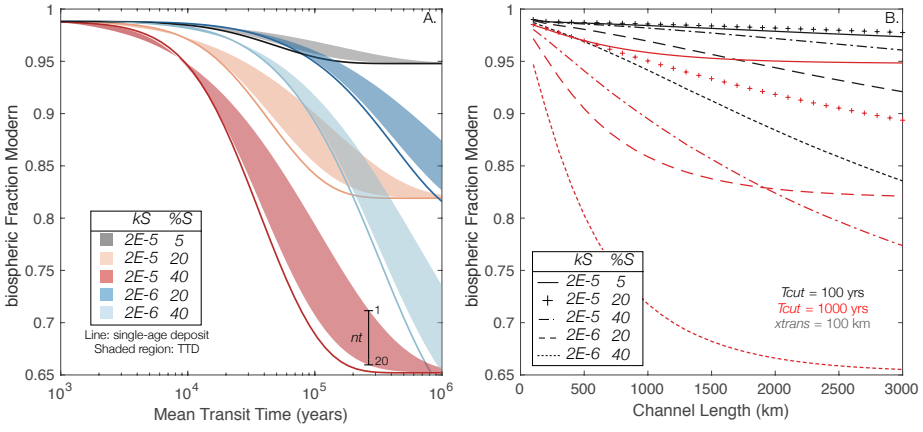

Figure 4. Model predictions of the radiocarbon content of POC. (a) Predicted relationships between sediment mean transit times (MTTs) and the Fm of biospheric POC for POC cycling models with variable proportions of slow POC ($\%S$) and variable slow POC consumption rate constants (kS). The Fm values shown as shaded areas were calculated using sediment transit time distributions (TTDs) with shapes set by between 1 to 20 transport events (Figure 3) and MTTs between 10^3 and 10^6 years. The model results show that plausible sediment TTDs yield significantly different relationships between the MTT and Fm relative to predictions for systems with a single transit time (solid bold lines). While TTD shape is an important factor reflected in the vertical range of each shaded area, the model results suggest that large differences of OC cycling (different colors; see figure legend) are distinguishable in the relationships between the MTT and Fm. (b) Predicted downstream profiles of Fm for a fixed x_{tran} (100 km), but variable T_{cut} (100 and 1000 years) and POC cycling parameters (different line styles; see figure legend). The model results suggest that observed downstream profiles are sensitive to both sediment storage timescales, which are controlled by T_{cut}, as well as OC cycling parameters.

Earth Surf. Dynam. Discuss., doi:10.5194/esurf-2017-29, 2017
Manuscript under review for journal Earth Surf. Dynam.
Discussion started: 15 May 2017

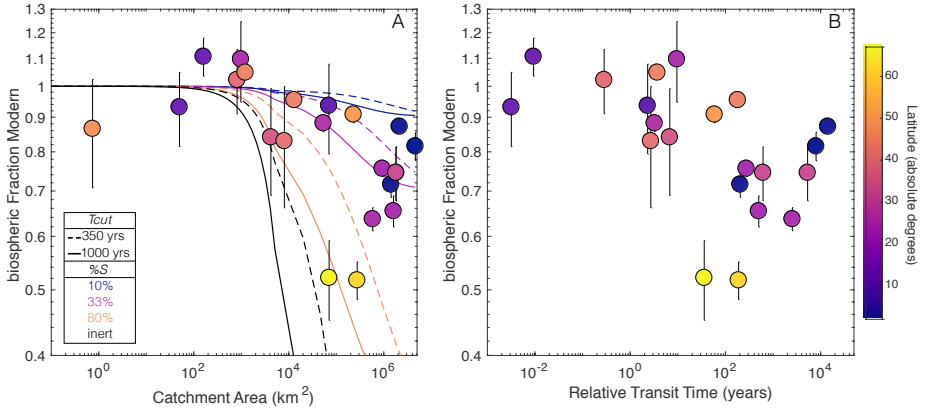

Figure 5. Field data compilation and comparison with model predictions. Field data are color coded based on their latitude as a proxy for POC cycling rates. (a) Model curves and field measurements of the relationship between catchment area and bulk biospheric Fm. Model curves are drawn for fixed POC consumption rate constants, but variable steady-state proportions of "slow" cycling POC and T_{cut} values (see legend). (b) Measured biospheric Fm values compared to our relative transit time metric (Equation 16), which is based on Hack's Law (Hack, 1957) and scaling relationships shown in Figures 2 and 3. The field data are consistent with the model predictions of aged POC in rivers with larger catchment areas and slower migration rates (inferred from variations in w^3/Q_s) and thus longer sediment storage times. We note that in our compilation of rivers with measurements of biospheric Fm, catchment area and w^3/Q_s are correlated.

Earth Surf. Dynam. Discuss., doi:10.5194/esurf-2017-29, 2017
Manuscript under review for journal Earth Surf. Dynam.
Discussion started: 15 May 2017

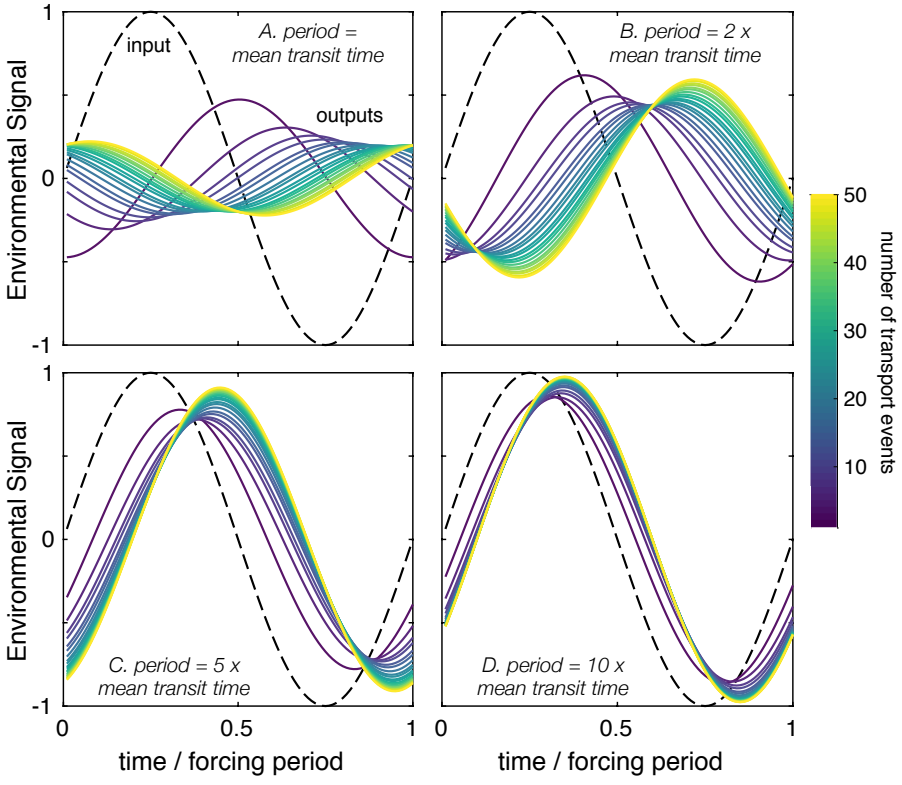

Figure 6. Effect of floodplain storage on environmental signals recorded by organic biomarkers. This figure shows the effect of convolving our sediment transit time distributions with a sine wave where the period of the sinusoidal input is equal to the mean transit time (a), twice the mean transit time (b), five times the mean transit time (c), and 10 times the mean transit time (d). The amplitude and phase of the sinusoidal input is shown as the black dashed lines. The colored lines refer to the output signal with the color reflecting the number of transport events (see color bar), which sets the shape of the transit time distribution. The model results suggest that climate signals recorded in terrestrial biomarkers will be significantly modulated if their period is short relative to the mean sediment transit time.

Earth Surf. Dynam. Discuss., doi:10.5194/esurf-2017-29, 2017
Manuscript under review for journal Earth Surf. Dynam.
Discussion started: 15 May 2017

Earth Surface Dynamics Discussions
Open Access
EGU

List of Tables

1 List of all rivers and their associated citations included in the radiocarbon compilation 39
2 Physical characteristics and inferred biospheric Fm values for a subset of rivers in the radiocarbon compilation 40

Earth Surf. Dynam. Discuss., doi:10.5194/esurf-2017-29, 2017
Manuscript under review for journal Earth Surf. Dynam.
Discussion started: 15 May 2017

Earth Surface Dynamics Discussions
Open Access
EGU

Table 1. List of all rivers and their associated citations included in the radiocarbon compilation

River	Citation
Alsea	Hatten et al. (2012)
Amazon	Bouchez et al. (2010, 2014)
Arctic Red	Hilton et al. (2015)
Atchafalaya	Gordon and Goni (2003); Rosenheim et al. (2013)
Avon	Adams et al. (2015)
Beni	Bouchez et al. (2010)
Brahmaputra	Galy et al. (2007)
Calder River	Adams et al. (2015)
Changjiang (Yangtze)	Wang et al. (2012); Li et al. (2015)
Chontabamba	Townsend-Small et al. (2007)
Chorobamba	Townsend-Small et al. (2007)
Conwy	Adams et al. (2015)
Dee	Adams et al. (2015)
Eel	Leithold et al. (2006)
Erlenbach	Smith et al. (2013); Turowski et al. (2016)
Esperanza	Townsend-Small et al. (2007)
Fly	Alin et al. (2008)
Fraser	Voss (2014)
Ganges	Galy et al. (2007)
Garin	Adams et al. (2015)
Hodder	Adams et al. (2015)
Huancabamba	Townsend-Small et al. (2007)
Kosi	Galy et al. (2007)
Kosñipata	Clark et al. (2013)
Lanyan Hsi	Kao and Liu (1996)
Liard	Hilton et al. (2015)
Liwu	Hilton et al. (2010)
Llamaquiz	Townsend-Small et al. (2007)
Madiera	Bouchez et al. (2010, 2014)
Meghna	Galy et al. (2007)
Mekong	Martin et al. (2013)
Mississippi	Rosenheim et al. (2013)
Narayani	Galy et al. (2007)
Navarro	Leithold et al. (2006)
Noyo	Leithold et al. (2006)
Peel	Hilton et al. (2015)
Pozuzo	Townsend-Small et al. (2007)
Rhône	Cathalot et al. (2013)
Ribble	Adams et al. (2015)
Santa Clara	Masiello and Druffel (2001); Komada et al. (2004)
Siuslaw	Leithold et al. (2006)
Solimoes	Bouchez et al. (2010, 2014)
Strickland	Alin et al. (2008)
Tokachi	Nagao et al. (2005)
Umpqua	Goñi et al. (2013)
Waiapu	Leithold et al. (2006)
Waipaoa	Leithold et al. (2006)
Yellow (Huanghe)	Wang et al. (2012); Tao et al. (2015); Hu et al. (2015)
Zengjiang	Gao et al. (2007)

Earth Surf. Dynam. Discuss., doi:10.5194/esurf-2017-29, 2017
Manuscript under review for journal Earth Surf. Dynam.
Discussion started: 15 May 2017

Earth Surface Dynamics Discussions
Open Access
EGU

Table 2. Physical characteristics and inferred biospheric Fm values for a subset of rivers in the radiocarbon compilation

River	Sediment Flux (Mt/yr)	Width (m)	Catchment Area (km^2)	Biospheric Fm	σ	Additional Data Source
Alsea	0.07	65	1220	1.05	0.01	USGS
Amazon	785	4767	4618750	0.82	0.04	HYBAM
Beni	212	410	69980	0.94	0.14	Wittmann et al. (2015)
Brahmaputra	540	4052	583000	0.64	0.03	
Changjiang	472	2000	1810000	0.75	0.07	Google Earth
Eel	14.00	250	8063	0.83	0.17	USGS
Erlenbach	0.001	5	0.74	0.87	0.16	Nitsche et al. (2012)
Fraser	20	450	230000	0.91	0.03	Google Earth
Ganges	660	1910	935000	0.76	0.02	
Kosi	135	412	53610	0.88	0.03	Google Earth
Kosñipata A	0.06	10	50	0.93	0.12	
Kosñipata B	0.18	17	160	1.11	0.07	
Lanyan Hsi	2.90	320	980	1.10	0.15	Google Earth
Liard	46	850	275000	0.52	0.03	Google Earth
Madiera	433	1401	1420000	0.72	0.03	Google Earth
Meghna	0.24	2600	1600000	0.65	0.03	Google Earth
Navarro	0.56	59	816	1.02	0.11	USGS
Peel	21	470	70600	0.52	0.07	Google Earth
Rhône	31	460	99000	1.41	0.15	Google Earth
Santa Clara	6.84	298	4200	0.84	0.15	USGS
Solimoes	569	5893	2147740	0.87	0.02	HYBAM
Umpqua	1.4	435	13000	0.95	0.02	USGS